ENERGY INJECTION FOR MECHANICAL SYSTEMS THROUGH THE METHOD
OF VIRTUAL NONHOLONOMIC CONSTRAINTS

by

Adan Moran-MacDonald

A thesis submitted in conformity with the requirements
for the degree of Master of Applied Science
Graduate Department of Electrical and Computer Engineering
University of Toronto

Abstract

Energy injection for mechanical systems through the method of Virtual Nonholonomic Constraints

Adan Moran-MacDonald

Master of Applied Science

Graduate Department of Electrical and Computer Engineering

University of Toronto

2020

TODO: Fill in the abstract

For Fry.

Acknowledgements

TODO: Fill in the acknowledgements

Contents

List of Symbols

Symbol	Definition
$\mathbf{n}$	The index set $\{1, \dots, n\}$ of natural numbers up to n.
$\mathbb{R}^n$	Real numbers in n dimensions.
$[\mathbb{R}]_T$	Real numbers modulo $T > 0$, with $[\mathbb{R}]_\infty = \mathbb{R}$.
$\mathbb{S}^1$	The unit circle, equivalent to $[\mathbb{R}]_{2\pi}$.
$\mathcal{Q}$	The configuration manifold of a system.
$C^r(X; Y)$	The space of r-times continuously differentiable functions from X to Y. If $r = \infty$, the space of smooth functions from X to Y.
$\mathbb{R}^{n \times m}$	The space of real-valued matrices with n rows and m columns.
I_n	The $n \times n$ identity matrix.
$\mathbf{0}_{n \times m}$	The $n \times m$ matrix of all zeros.
M_i	If M is a vector, the ith element of M. If M is a matrix, the ith column of M.
$M_{i,j}$	The value of row i, column j for the matrix M.
$\dot{x}$	Derivative of x with respect to time t.
$\nabla_v F$	If F is $\mathbb{R}$-valued, the gradient of F with respect to v. If F is $\mathbb{R}^{n \times n}$-valued and $v \in \mathbb{R}^m$, the block gradient $\left[\nabla_{v_1} F^{\mathsf{T}} \dots \nabla_{v_m} F^{\mathsf{T}} \right]^{\mathsf{T}} \in \mathbb{R}^{nm \times n}$.
dF_v	Total differential (Jacobian) of F, equivalent to $(\nabla_v F)^{\mathsf{T}}$.
$\operatorname{Hess} F$	If $F : \mathbb{R}^n \to \mathbb{R}$, the $n \times n$ Hessian matrix of double derivatives of F. If $F : \mathbb{R}^n \to \mathbb{R}^k$, the block matrix $(\operatorname{Hess} F_1, \dots, \operatorname{Hess} F_k) \in \mathbb{R}^{n \times nk}$.
$\partial_v \partial_w F$	Derivative matrix of $F : \mathbb{R}^n \times \mathbb{R}^m \to \mathbb{R}$, with (i, j) element $\frac{\partial^2 F}{\partial v_i \partial w_j}$.
$\delta_{i,j}$	The Kronecker delta: 1 if $i = j$ and 0 otherwise.
$\otimes$	The matrix kronecker product.
$\lVert \cdot \rVert$	The euclidean norm on $\mathbb{R}^n$.

TEST CITATIONS:

[1] [2] [3] [4] [5] [6] [7] [8] [9] [10] [11] [12] [13] [14] [15] [16] [17] [18] [19] [20] [21] [22] [23] [24] [25] [26] [27] [28] [29] [30] [31] [32] [33] [34] [35] [36] [37] [38] [39] [40] [41] [42] [43] [44] [45] [46] [47] [48] [49] [50] [51] [52] [53]

Chapter 1

Introduction

1.1   Literature Review

1.2   Statement of Contributions

**1.3   Outline of the Thesis**

1.4   Notation

Chapter 2

Development of Virtual Nonholonomic Constraints

## 2.1   Preliminaries on Analytical Mechanics

A mechanical system can be represented by N point masses where each point represents the center of mass of a physical body, along with r *equations of constraint* (EOC) which model the physical restrictions between these masses. The position of each point mass is described using three cartesian coordinates (one for each spatial axis), so the system as a whole can be described by a vector in $\mathbb{R}^{3N}$ with r EOC. The dynamics of the system are computed by deriving the $3N$ *equations of motion* (EOM) produced by Newton's second law $F = ma$. While this technique works for simple systems, it is tedius and becomes impossible to apply to complex mechanical systems where the forces are not explicitly known.

Rather than modeling a mechanical system by cartesian positions and constraints, it is often feasible to represent the position of the system using n independent scalar-valued variables $q_1, \dots, q_n$ called *generalized coordinates*, where $n = 3N - r$ is the number of *degrees of freedom* (DOF) of the system [23]. For instance, Figure 2.1 shows a barbell on a 2*D*-plane which can rotate freely on that plane. The barbell has $n = 3$ DOF, so it can be described by three independent generalized coordinates with no equations of constraint.

For the robotic systems of interest in this thesis, we assume that each generalized coordinate q_i represents either the distance or the angle between two parts of the system. Mathematically, each q_i takes values in $[\mathbb{R}]_{T_i}$, where $T_i = \infty$ if q_i represents a length or $T_i = 2\pi$ if q_i represents an angle. It is convention to collect the coordinates into a
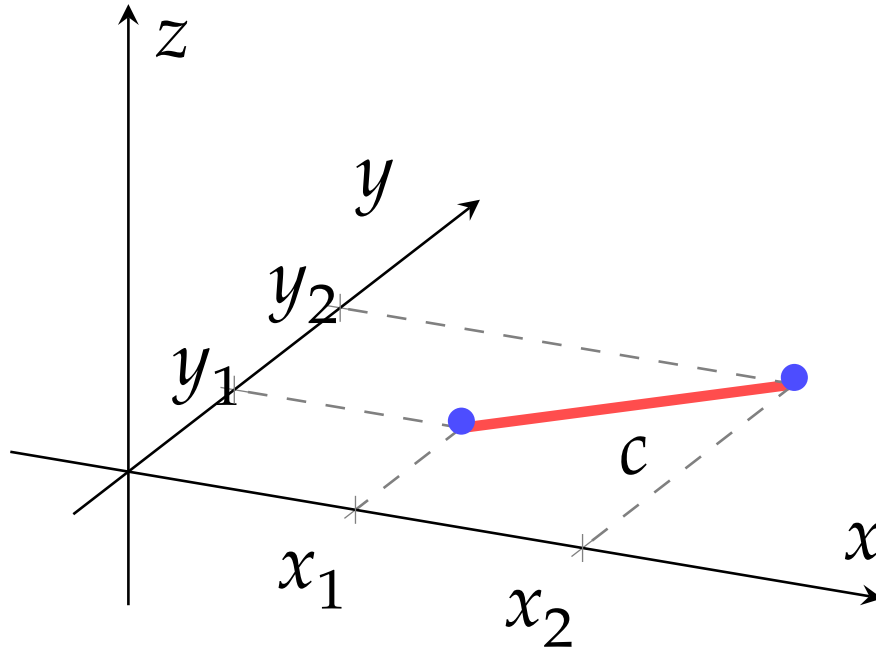
(A) The Newtonian representation of the barbell requires all six cartesian positions and the corresponding EOC.
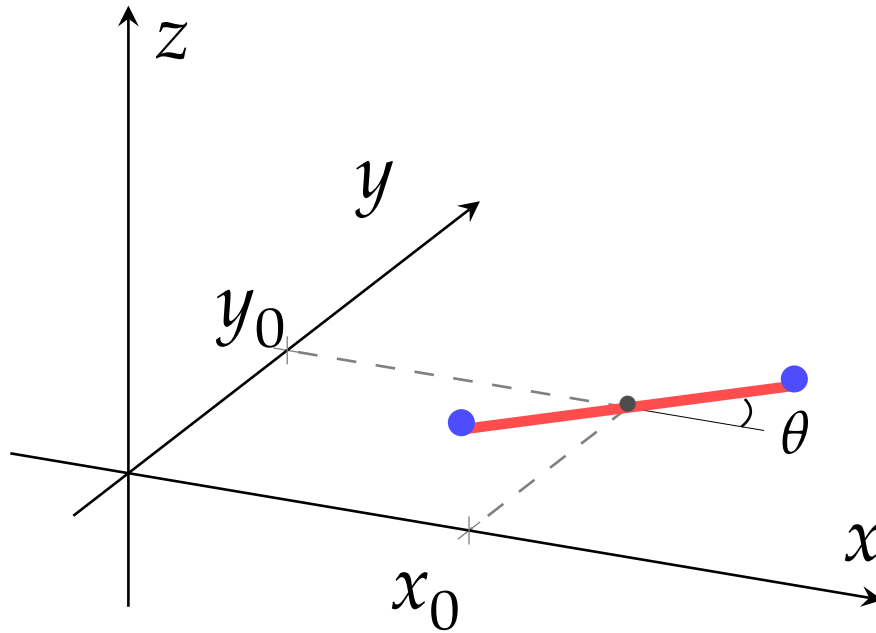
(B) One possible set of three generalized coordinates is (x_0, y_0, θ), which represent the position of the center of the bar and the angle of the barbell in the xy-plane.

FIGURE 2.1: A mechanical system with $N = 2$ point masses at $a = (x_1, y_1, z_1)$ and $b = (x_2, y_2, z_2)$, separated by a bar of length c. There are $r = 3$ EOC given by $\|a - b\| = c$, $z_1 = 0$, and $z_2 = 0$. This system has $n = 3$ degrees of freedom.

configuration $q = (q_1, \ldots, q_n) \in \mathcal{Q}$ where the *configuration manifold* $\mathcal{Q}$ of the system is a so-called *generalized cylinder*

$$\mathcal{Q} = [\mathbb{R}]_{T_1} \times \cdot \times [\mathbb{R}]_{T_n}.$$

The derivative $\dot{q} = (\dot{q}_1, \ldots, \dot{q}_n)$ of a configuration is called a *generalized velocity* of the system. For arbitrary systems, the space of allowable velocities depends on the current configuration of the system. However, since $\mathcal{Q}$ is a generalized cylinder, we find that $\dot{q} \in \mathbb{R}^n$. The combined vector $(q, \dot{q}) \in \mathcal{Q} \times \mathbb{R}^n$ is called a *state* of the system.

The field of analytical mechanics provides a computational method for finding the EOM of a system in generalized coordinates. The two most common analytical methods for modelling robotic systems are *Lagrangian* and *Hamiltonian* mechanics.

2.1.1 Lagrangian Mechanics

Lagrangian mechanics uses the kinetic energy $T(q, \dot{q})$ and potential energy $P(q)$ of the system to define the Lagrangian $\mathscr{L} : \mathcal{Q} \times \mathbb{R}^n \to \mathbb{R}$ defined by (2.1) [23],

$$\mathscr{L}(q, \dot{q}) = T(q, \dot{q}) - P(q). \tag{2.1}$$

When the mechanical system is actuated, the EOM are described by n second-order ordinary differential equations (ODEs) obtained from the *Euler-Lagrange equations* (2.2) with *generalized input forces* $\tau \in \mathbb{R}^k$

$$\frac{d}{dt}\left\{\frac{\partial \mathscr{L}}{\partial \dot{q}_i}\right\} - \frac{\partial \mathscr{L}}{\partial q_i} = B_i^{\mathsf{T}}(q)\tau. \tag{2.2}$$

The vector $B_i^{\mathsf{T}} : \mathcal{Q} \to \mathbb{R}^{1 \times k}$ describes how the input forces shape the dynamics of q_i. The matrix $B : \mathcal{Q} \to \mathbb{R}^{n \times k}$ with

$$B(q) = \begin{bmatrix} - & B_1^{\mathsf{T}}(q) & - \\ & \vdots & \\ - & B_n^{\mathsf{T}}(q) & - \end{bmatrix},$$

is called the *input matrix* for the system. If $k < n$, we say the system is *underactuated* with degree of underactuation $(n - k)$.

Many actuated mechanical systems have quadratic kinetic energies, so that the Lagrangian can be written explicitly as

$$\mathscr{L}(q, \dot{q}) = \frac{1}{2}\dot{q}^{\mathsf{T}}D(q)\dot{q} - P(q), \tag{2.3}$$

where the *inertia matrix* $D : Q \rightarrow \mathbb{R}^{n \times n}$ is a symmetric, positive definite matrix for all $q \in Q$ and the potential function $P : Q \rightarrow \mathbb{R}$ is smooth.

2.1.2   Hamiltonian Mechanics

Hamiltonian mechanics converts the n second-order ODEs generated by Lagrangian mechanics into an equivalent set of $2n$ first-order ODEs.

To do this, we first define the *conjugate of momentum p_i to q_i* by

$$p_i(q, \dot{q}) := \frac{\partial \mathscr{L}}{\partial \dot{q}_i}(q, \dot{q}). \tag{2.4}$$

To ease notation, we write $p = (p_1, \dots, p_n) \in \mathbb{R}^n$ and call p the *conjugate of momenta to q*. Note that each p_i is a linear function of $\dot{q}$, and one can typically solve for $\dot{q}(q, p)$ by inverting all the expressions from (2.4). The combined vector $(q, p) \in Q \times \mathbb{R}^n$ is called a *phase* of the system.

The *Hamiltonian* of the system in (q, p) coordinates is the "Legendre transform" (2.5) of the Lagrangian [24],

$$\mathscr{H}(q, p) := p^\mathsf{T} \dot{q}(q, p) - \mathscr{L}(q, \dot{q}(q, p)). \tag{2.5}$$

The EOM in the Hamiltonian framework are the $2n$ first-order equations called *Hamilton's equations*. They are given by

$$\begin{cases} \dot{q} = \nabla_p \mathscr{H} \\ \dot{p} = -\nabla_q \mathscr{H} + B(q)\tau. \end{cases} \tag{2.6}$$

Here, $B(q) \in \mathbb{R}^{n \times k}$ is the same input matrix used by the Lagrangian framework, with $\tau \in \mathbb{R}^k$ the same vector of generalized input forces.

If the kinetic energy of the system is quadratic as in (2.3), the conjugate of momenta becomes $p = D(q)\dot{q}$. Since $D(q)$ is symmetric and positive definite, it is invertible at each $q \in Q$. The Legendre transform (2.5) becomes

$$\mathscr{H}(q, p) = p^\mathsf{T} D^{-1}(q)p - \left(\frac{1}{2} p^\mathsf{T} D^{-1}(q)p - P(q) \right)$$
$$= \frac{1}{2} p^\mathsf{T} D^{-1}(q)p + P(q).$$

Finding the derivative of each momentum coordinate yields

$$\dot{p}_i = -\frac{1}{2}p^\mathsf{T}\nabla_{q_i}D^{-1}(q)p - \frac{\partial P}{\partial q_i}(q) + B_i^\mathsf{T}(q)\tau.$$

Recall the Kronecker product of matrices [51], defined as follows.

Definition 2.1. Let $A \in \mathbb{R}^{n \times m}$ and $B \in \mathbb{R}^{r \times s}$. The Kronecker product $A \otimes B \in \mathbb{R}^{nr \times ms}$ is the matrix

$$A \otimes B = \begin{bmatrix} a_{1,1}B & \cdots & a_{1,m}B \\ \vdots & \ddots & \vdots \\ a_{n,1}B & \cdots & a_{n,m}B \end{bmatrix}.$$

Using the kronecker product, one can collect the derivative of momentum into the vector form

$$\dot{p} = -\frac{1}{2}(I_n \otimes p^\mathsf{T})\nabla_q D^{-1}(q)p - \nabla_q P(q) + B(q)\tau.$$

In sum, when the kinetic energy is quadratic the Hamiltonian system reduces to

$$\mathcal{H}(q,p) = \frac{1}{2}p^\mathsf{T}D^{-1}(q)p + P(q), \tag{2.7}$$

$$\begin{cases} \dot{q} = D^{-1}(q)p \\ \dot{p} = -\frac{1}{2}(I_n \otimes p^\mathsf{T})\nabla_q D^{-1}(q)p - \nabla_q P(q) + B(q)\tau. \end{cases} \tag{2.8}$$

Any set of coordinates (q, p) which satisfy Hamilton's equations under the Hamiltonian $\mathcal{H}$ are said to be *canonical coordinates* for the system. A change of coordinates $(q, p) \to (Q, P)$ is a *canonical transformation* if (Q, P) preserve the Hamiltonian structure; that is, if they are canonical coordinates under the Hamiltonian $\mathcal{H}\left(q(Q, P), p(Q, P)\right)$.

Landau and Lifschitz [24] provide a useful result for showing whether a given change of coordinates $(q, p) \to (Q, P)$ is a canonical transformation.

Definition 2.2. The *Poisson bracket* between the functions $f(q, p)$ and $g(q, p)$ is

$$[f, g] := \sum_{i=1}^{n} \frac{\partial f}{\partial p_i}\frac{\partial g}{\partial q_i} - \frac{\partial f}{\partial q_i}\frac{\partial g}{\partial p_i}. \tag{2.9}$$

Theorem 2.3. *A change of coordinates* $(q, p) \to (Q, P)$ *is a canonical transformation if and*

only if

$$[Q_i, Q_j] = 0,$$
$$[P_i, P_j] = 0,$$
$$[P_i, Q_j] = \delta_{i,j},$$

for all $i, j \in \mathbf{n}$.

Proof. See (45.10) in [24]. ☐

Later in this chapter we will define a particular change of coordinates. The following Lemma allows us to prove it is a canonical transformation.

Lemma 2.4. *Let $\mathcal{H}$ be a Hamiltonian system in canonical coordinates (q, p). Let $A \in \mathbb{R}^{n \times n}$ be an orthogonal matrix. The change of coordinates $(q, p) \to (Q = Aq, P = Ap)$ is a canonical transformation.*

Proof. For any constant matrix A, the transformation $(Q = Aq, P = Ap)$ satisfies $\frac{\partial Q_i}{\partial p_m} = \frac{\partial P_i}{\partial q_m} = 0$ for all $i, m \in \mathbf{n}$. Hence,

$$[Q_i, Q_j] = \sum_{m=1}^{n} \frac{\partial Q_i}{\partial p_m} \frac{\partial Q_j}{\partial q_m} - \frac{\partial Q_i}{\partial q_m} \frac{\partial Q_j}{\partial p_m} = 0,$$
$$[P_i, P_j] = \sum_{m=1}^{n} \frac{\partial P_i}{\partial p_m} \frac{\partial P_j}{\partial q_m} - \frac{\partial P_i}{\partial q_m} \frac{\partial P_j}{\partial p_m} = 0.$$

Note that $(A_i)^\mathsf{T}(A^\mathsf{T})_j = (A_i)^\mathsf{T}(A^{-1})_j = \delta_{i,j}$. Using this fact we see that the Poisson brackets between P_i and Q_j are given by

$$
\begin{aligned}
[P_i, Q_j] &= \sum_{m=1}^{n} \frac{\partial P_i}{\partial p_m} \frac{\partial Q_j}{\partial q_m} - \frac{\partial P_i}{\partial q_m} \frac{\partial Q_j}{\partial p_m} \\
&= \sum_{m=1}^{n} A_{i,m} A_{j,m} - 0 \\
&= \sum_{m=1}^{n} A_{i,m} (A^\mathsf{T})_{m,j} \\
&= (A_i)^\mathsf{T} (A^\mathsf{T})_j \\
&= \delta_{i,j}.
\end{aligned}
$$

Therefore, by Theorem 2.3, the coordinate change $(Q = Aq, P = Ap)$ is a canonical transformation. ☐

2.2 Simply Actuated Hamiltonian Systems

Suppose we are given a Hamiltonian mechanical system (2.7). Because τ is transformed by the input matrix $B(q)$ before entering the EOM, it is not in general clear how any particular input force τ_i will affect the dynamics of the system. In this section, we define a new class of Hamiltonian systems where the effect of the input forces is made obvious. This class of systems will form the backbone for the rest of the theory developed in this thesis.

Definition 2.5. Let $\mathscr{H}$ be an n-DOF Hamiltonian system with $k \leq n$ actuators. A set of canonical coordinates (q, p) for this system are said to be *simply actuated coordinates* if the input matrix $B(q) \in \mathbb{R}^{n \times k}$ is of the form

$$B(q) = \begin{bmatrix} \mathbf{0}_{(n-k) \times k} \\ I_k \end{bmatrix}.$$

The first $(n-k)$ coordinates, labelled q_u, are called the *unactuated coordinates*. The remaining k coordinates, labelled q_a, are called the *actuated coordinates*. When grouping them together, we will always put them in the order (q_u, q_a) to fit with the definition. The corresponding (p_u, p_a) are called the *unactuated* and *actuated momenta*, respectively.

Under the following assumptions on the input matrix, we will show that there is a canonical transformation of (2.7) into simply actuated coordinates.

Assumption 1. The input matrix $B(q) \equiv B \in \mathbb{R}^{n \times k}$ is constant, full rank, and $k < n$.

Assumption 2. There exists a matrix $B^{\perp} \in \mathbb{R}^{(n-k) \times n}$ which is right semi-orthogonal $\left(B^{\perp}(B^{\perp})^{\mathsf{T}} = I_{(n-k)} \right)$ and which is a left-annihilator for B. That is, $B^{\perp}B = \mathbf{0}_{(n-k) \times k}$.

Assumption 2 requires the rows of $B^{\perp}$ to be unit vectors that are mutually orthogonal. In the case that $k = (n-1)$, the existence of any left annihilator $A^0 \in \mathbb{R}^{1 \times n}$ implies the left annihilator $B^{\perp} := A^0 / \|A^0\|$ will be a unit vector satisfying Assumption 2.

Lemma 2.6. *Suppose Assumption 1 holds. Then there exists a nonsingular matrix $\hat{T} \in \mathbb{R}^{k \times k}$ so that the regular feedback transformation*

$$\tau = \hat{T}\hat{\tau}$$

has a new input matrix $\hat{B}$ for $\hat{\tau}$ which is left semi-orthogonal. That is, $\hat{B}^{\mathsf{T}}\hat{B} = I_k$.

Proof. Since B is a constant matrix, it has a singular-value decomposition $B = U\Sigma V^\mathsf{T}$ where $U^{-1} = U^\mathsf{T} \in \mathbb{R}^{n \times n}$, $V^{-1} = V^\mathsf{T} \in \mathbb{R}^{k \times k}$, and $\Sigma \in \mathbb{R}^{n \times k}$ is defined by

$$\Sigma = \begin{bmatrix} \sigma_1 & 0 & \cdots & 0 \\ 0 & \sigma_2 & \cdots & 0 \\ \vdots & & \ddots & \vdots \\ 0 & 0 & \cdots & \sigma_k \\ - & \mathbf{0}_{(n-k) \times k} & - \end{bmatrix},$$

where $\sigma_i \neq 0$ because B is full-rank [49]. Define $T \in \mathbb{R}^{k \times k}$ by

$$T = \begin{bmatrix} \frac{1}{\sigma_1} & 0 & \cdots & 0 \\ 0 & \frac{1}{\sigma_2} & \cdots & 0 \\ \vdots & & \ddots & \vdots \\ 0 & 0 & \cdots & \frac{1}{\sigma_k} \end{bmatrix}.$$

Letting $\hat{T} = VT$ and assigning the regular feedback transformation $\tau = \hat{T}\hat{\tau}$, we get a new input matrix for $\hat{\tau} \in \mathbb{R}^k$ given by

$$\hat{B} = B\hat{T} = BVT = U \begin{bmatrix} I_k \\ \mathbf{0}_{(n-k) \times k} \end{bmatrix},$$

which is still constant and full-rank. In particular, $\hat{B}^\mathsf{T}\hat{B} = T^\mathsf{T}\Sigma^\mathsf{T}\Sigma T = I_k$. □

In light of Lemma 2.6, there is no loss of generality by making the following assumption.

Assumption 3. Assume that the input matrix B is left semi-orthogonal, *i.e.*, $B^\mathsf{T}B = I_k$.

Let now $\mathbf{B} \in \mathbb{R}^{n \times n}$ be the following matrix:

$$\mathbf{B} = \begin{bmatrix} B^\perp \\ B^\mathsf{T} \end{bmatrix}.$$

Since $B^\perp$ is a left annihilator of B and both $B^\perp$ and B^T are right semi-orthogonal, it is easy to show that $\mathbf{B}$ is orthogonal.

Proof.

$$\mathbf{B}\mathbf{B}^\mathsf{T} = \begin{bmatrix} B^\perp (B^\perp)^\mathsf{T} & B^\perp B \\ (B^\perp B)^\mathsf{T} & B^\mathsf{T} B \end{bmatrix} = I_n.$$

Hence, $\mathbf{B}$ is invertible with $\mathbf{B}^{-1} = \mathbf{B}^{\mathsf{T}}$.   □

The following theorem shows that $\mathbf{B}$ provides a canonical transformation into simply actuated coordinates, so that only the actuated momenta are affected by the input forces.

Theorem 2.7. *Under Assumptions 1,2, and 3, the Hamiltonian system (2.7) has simply actuated canonical coordinates* $(Q = \mathbf{B}q, P = \mathbf{B}p)$. *The resulting dynamics are given by (2.10),*

$$\mathscr{H}(Q,P) = \frac{1}{2}P^{\mathsf{T}}M^{-1}(Q)P + V(Q), \tag{2.10}$$

$$\begin{cases} \dot{Q} = M^{-1}(Q)P \\ \dot{P} = -\frac{1}{2}(I_n \otimes P^{\mathsf{T}})\nabla_Q M^{-1}(Q)P - \nabla_Q V(Q) + \begin{bmatrix} \mathbf{0}_{(n-k)\times k} \\ I_k \end{bmatrix}\tau, \end{cases}$$

where

$$M^{-1}(Q) := \mathbf{B}D^{-1}(\mathbf{B}^{\mathsf{T}}Q)\mathbf{B}^{\mathsf{T}},$$
$$V(Q) := P(\mathbf{B}^{\mathsf{T}}Q).$$

Proof. The change of coordinates $(Q = \mathbf{B}q, P = \mathbf{B}p)$ satisfies Lemma 2.4, making it a canonical transformation. Furthermore, since $\dot{P} = \mathbf{B}\dot{p}$, the new input matrix is given by

$$\mathbf{B}B = \begin{bmatrix} B^{\perp}B \\ B^{\mathsf{T}}B \end{bmatrix} = \begin{bmatrix} \mathbf{0}_{(n-k)\times k} \\ I_k \end{bmatrix},$$

which means $(Q = (q_u, q_a), P = (p_u, p_a))$ are simply actuated coordinates for $\mathscr{H}$ as desired.   □

2.3   Virtual Nonholonomic Constraints

Let us imagine a child on a swing who wants to reach the largest height possible. To begin, the child pushes off the ground to imbue the swing with small oscillations. What allows them to increase the amplitude of these oscillations is the appropriate extension and retraction of their feet. If a roboticist were creating a machine to replicate this behaviour, they might design a robot whose legs extend and retract at specific time intervals. At first glance, this technique should work perfectly because the leg motion would synchronize with the swinging frequency, thereby injecting energy as quickly as is physically possible.

Unfortunately, a deeper analysis reveals the flaw with this design. Most children are not counting out the time in their head; rather, they observe their current position and velocity and adjust their legs as required. For example, many children have an adult pushing the swing, or perhaps they are swinging on a windy day. In either case, they adjust their leg motion accordingly when presented with these external disturbances, without keeping track of time. Hence, the standard control technique of tracking a function of time (known as *trajectory tracking*) does not truly replicate human behaviour. Even if the robot's legs perfectly track a specified trajectory, an external disturbance will desynchronize the leg motion with the swing - thereby stopping the amplitude-increasing effects.

Rather than tracking a trajectory over time, a more human-like behaviour is to force the robot's legs track a function of the swing's state. One recent control method known as *virtual holonomic constraints* (VHCs) uses the actuators to enforce a relation $h(q) = 0$ of the configuration [19]. This method has provided incredible results in the development of walking robots [27, 28], vehicle motion [30, 31], and has even been used to design a snake-like swimming robot [29].

The downside to VHCs is that they only depend on the configuration of a mechanical system, and not its generalized velocity. For the child on a swing, whether they extend or retract their legs depends on their direction of motion. This inherently requires knowledge of their current velocity, which precludes the usage of VHCs. A few authors have attempted to extend the theory of VHCs to enforce relations $h(q, \dot{q}) = 0$ of the full state to account for this drawback. Since these relations use actuators to restrict both the configuration and velocity of a system, they are called virtual *nonholonomic* constraints. This idea has been used for human-robot interaction [32–34], error-reduction on time-delayed systems [35], and has shown marked improvements to the field of bipedal locomotion [9, 36, 38]. Most interestingly, this nonholonomic approach is more robust than standard VHCs when applied to bipedal robotics [37]. In particular, virtual nonholonomic constraints may be capable of injecting and dissipating energy from a system in a robust manner, all while producing realistic biological motion. This is what we aim to prove in this thesis.

Unlike the theory of VHCs, there does not appear to be a standard definition of virtual nonholonomic constraints: all the applications listed above use their own definitions, which makes it difficult to compare and generalize their work.

This section will provide a standard characterization of virtual nonholonomic constraints using Hamiltonian mechanics. The goal is to provide a consistent, rigorous foundation for designing constraints on a general class of systems.

Definition 2.8. A *virtual nonholonomic constraint* (VNHC) *of order* k is a relation $h(q, p) = 0$ where $h : \mathcal{Q} \times \mathbb{R}^n \to \mathbb{R}^k$ is C^2, rank $\left(\left[dh_q, dh_p \right] \right) = k$ for all $(q, p) \in h^{-1}(0)$, and there exists a feedback controller $\tau(q, p)$ rendering the *constraint manifold* Γ invariant where

$$\Gamma = \left\{ (q, p) \mid h(q, p) = 0, dh_q \dot{q} + dh_p \dot{p} = 0 \right\}.$$

From the definition of VNHCs, one finds that the constraint manifold Γ is a $2(n - k)$-dimensional closed embedded submanifold of $\mathcal{Q} \times \mathbb{R}^n$. The next obvious question is the following: when does a feedback controller stabilizing Γ exist?

One approach to answering this question is to define the error term $e = h(q, p)$. If there exists some controller $\tau(q, p)$ driving $e \to 0$ and $\dot{e} \to 0$, then the same τ will necessarily stabilize Γ (under additional mild conditions, see [19]) [1].

We say that e is of *relative degree* $\{r_1, \dots, r_k\}$ if

1. Some component of τ appears at the r_i^{th} derivative of e_i for $i \in \{1, \dots, k\}$.

2. In the vector of time-derivatives $(e_1^{(r_1)}, \dots, e_k^{(r_k)})$, the vector τ is premultiplied by a nonsingular matrix.

With no further structure on $h(q, p)$, the control input τ usually appears after one derivative of e; unfortunately, if any e_i has relative degree $r_i = 1$ we may not be able to stabilize Γ. We could guarantee $e_i(t) \to 0$, but we could not in general guarantee $\dot{e}_i(t) \to 0$.

Requiring e to have relative degree $\{2, \dots, 2\}$ is much more useful, since it allows us to easily solve for a controller stabilizing Γ. This kind of relative degree requirement is already common in the VHC literature. Taking advantage of that precedent, we define a special type of VNHC that satisfies this property.

Definition 2.9. A VNHC $h(q, p) = 0$ of order k is *regular* if the output $e = h(q, p)$ is of relative degree $\{2, 2. \dots, 2\}$ everywhere on the constraint manifold Γ.

The authors of [9, 36, 37] observed that a relation which uses only the unactuated conjugate of momentum cannot have τ appearing after only one derivative. Of course, they performed their research in Lagrangian form; we will be using the Hamiltonian formulation from Chapter 2.2. As a reminder, our system is described in (q, p) coordinates

---

[1] The type of constraints we consider in this thesis are graphs of functions, and so meet these mild assumptions.

with $q = (q_u, q_a)$ and $p = (p_u, p_a)$ and has the dynamics

$$\mathcal{H}(q, p) = p^\mathsf{T} M^{-1}(q) p + V(q), \tag{2.11}$$

$$\begin{cases} \dot{q} = M^{-1} p \\ \dot{p} = -\frac{1}{2}(I_n \otimes p^\mathsf{T}) \nabla_q M^{-1}(q) p - \nabla_q V(q) + \begin{bmatrix} \mathbf{0}_{(n-k) \times k} \\ I_k \end{bmatrix} \tau. \end{cases} \tag{2.12}$$

Notation. We will write $q_u \in \mathcal{Q}_u$, $q_a \in \mathcal{Q}_a$ where $\mathcal{Q}_u \times \mathcal{Q}_a = \mathcal{Q}$. We also write $p_u \in \mathcal{P}_u :=$ $\mathbb{R}^{n-k}$ and $p_a \in \mathcal{P}_a := \mathbb{R}^k$, so that $p \in \mathcal{P} := \mathcal{P}_u \times \mathcal{P}_a = \mathbb{R}^n$. In this manner, the phase space of our system can be written as $\mathcal{Q} \times \mathcal{P}$.

Theorem 2.10. *A relation $h(q, p) = 0$ for system (2.11) is a regular VNHC of order k if and only if $dh_{p_a} = 0$ and*

$$\mathrm{rank}\left(\left(dh_q M^{-1}(q) - dh_{p_u}(I_{n-k} \otimes p^\mathsf{T}) \nabla_{q_u} M^{-1}(q) \right) \begin{bmatrix} \mathbf{0}_{(n-k) \times k} \\ I_k \end{bmatrix} \right) = k,$$

everywhere on the constraint manifold Γ.

Proof. Let $e = h(q, p) \in \mathbb{R}^k$. Then

$$\dot{e} = dh_q \dot{q} + dh_p \dot{p}$$
$$= dh_q M^{-1}(q) p +$$
$$\begin{bmatrix} dh_{p_u} & dh_{p_a} \end{bmatrix} \left(-\frac{1}{2} \begin{bmatrix} (I_{n-k} \otimes p^\mathsf{T}) \nabla_{q_u} M^{-1}(q) p \\ (I_k \otimes p^\mathsf{T}) \nabla_{q_a} M^{-1}(q) p \end{bmatrix} - \begin{bmatrix} \nabla_{q_u} V(q) \\ \nabla_{q_a} V(q) \end{bmatrix} + \begin{bmatrix} \mathbf{0}_{(n-k) \times k} \\ I_k \end{bmatrix} \tau \right).$$

If $dh_{p_a} \neq \mathbf{0}_{k \times k}$ for some (q, p) on Γ, then τ appears in $\dot{e}$ and the VNHC is not of relative degree $\{2, 2, \dots, 2\}$. Hence, we must have that $dh_{p_a} = \mathbf{0}_{k \times k}$. Proceeding with this assumption, we now find that $h : \mathcal{Q} \times \mathcal{P}_u \to \mathbb{R}^k$, which means that

$$\dot{e} = dh_q M^{-1}(q) p - dh_{p_u} \left(\frac{1}{2}(I_{n-k} \otimes p^\mathsf{T}) \nabla_{q_u} M^{-1}(q) p + \nabla_{q_u} V(q) \right).$$

Taking one further derivative provides

$$
\ddot{e} = \left(\frac{d}{dt} dh_q \right) M^{-1}(q)p + dh_q \left(\sum_{i=1}^n \frac{\partial M^{-1}}{\partial q_i}(q)\dot{q}_i \right) p + dh_q M^{-1}(q)\dot{p} -
$$
$$
\left(\frac{d}{dt} dh_{p_u} \right) \left(\frac{1}{2}(I_{n-k} \otimes p^{\mathsf{T}}) \nabla_{q_u} M^{-1}(q)p + \nabla_{q_u} V(q) \right) -
$$
$$
dh_{p_u} \left(\frac{1}{2} \frac{d}{dt} \left((I_{n-k} \otimes p^{\mathsf{T}}) \nabla_{q_u} M^{-1}(q)p \right) + \left(\frac{d}{dt} \nabla_{q_u} V(q) \right) \right).
$$

Most of these terms do not involve $\dot{p}$ and hence do not contain τ, so we shorten this to

$$
\ddot{e} = (\star) - dh_{p_u} \left(\frac{1}{2} \frac{d}{dt} \left((I_{n-k} \otimes p^{\mathsf{T}}) \nabla_{q_u} M^{-1}(q)p \right) \right) + dh_q M^{-1}(q) \begin{bmatrix} \mathbf{0}_{(n-k)\times k} \\ I_k \end{bmatrix} \tau.
$$

Observe that the ith row of $\frac{1}{2}\frac{d}{dt} \left((I_{n-k} \otimes p^{\mathsf{T}}) \nabla_{q_u} M^{-1}(q)p \right)$ is given by

$$
\frac{1}{2} \frac{d}{dt} \left(p^{\mathsf{T}} \frac{\partial M^{-1}}{\partial q_{u_i}}(q)p \right) = p^{\mathsf{T}} \frac{\partial M^{-1}}{\partial q_{u_i}}(q)\dot{p} + \frac{1}{2} p^{\mathsf{T}} \left(\sum_{j=1}^n \frac{\partial^2 M^{-1}}{\partial q_{u_i} \partial q_j} \dot{q}_j \right) p.
$$

Highlighting only the term containing τ, we get the vector form

$$
\frac{1}{2}\frac{d}{dt} \left((I_{n-k} \otimes p^{\mathsf{T}}) \nabla_{q_u} M^{-1}(q)p \right) = (\star) + (I_{n-k} \otimes p^{\mathsf{T}}) \nabla_{q_u} M^{-1}(q) \begin{bmatrix} \mathbf{0}_{(n-k)\times k} \\ I_k \end{bmatrix} \tau.
$$

Plugging this into $\ddot{e}$ reveals that

$$
\ddot{e} = (\star) + \left(dh_q M^{-1}(q) - dh_{p_u}(I_{n-k} \otimes p^{\mathsf{T}}) \nabla_{q_u} M^{-1}(q) \right) \begin{bmatrix} \mathbf{0}_{(n-k)\times k} \\ I_k \end{bmatrix} \tau,
$$

where $(\star)$ is a continuous function of q and p. For shorthand, we'll write

$$
\ddot{e} = E(q,p) + H(q,p)\tau,
$$

where E and H are defined appropriately. From the definition of regularity, the VNHC h is regular when e is of relative degree $\{2,\ldots,2\}$, which is true if and only if the matrix premultiplying τ is nonsingular, and hence that H is invertible. This proves the theorem.

$\square$

Using the expression $\ddot{e} = E(q,p) + H(q,p)\tau$ from the proof of Theorem 2.10, a regular

VNHC of order k can be stabilized by[2] the output-linearizing phase-feedback controller

$$\tau(q,p) = -H^{-1}(q,p)\left(E(q,p) + k_p e + k_d \dot{e}\right),\tag{2.13}$$

where $k_p, k_d \in \mathbb{R}_{>0}$ are control parameters which can be tuned on the resulting linear system $\ddot{e} = -k_p e - k_d \dot{e}$.

Note that one generally cannot measure conjugate of momenta directly, as sensors on mechanical systems will only measure the state $(q, \dot{q})$. To implement this controller in practice, one must compute $p = M(q)\dot{q}$ at every iteration. In other words, this controller requires knowledge of the full state of the system.

Now that we have found a controller to enforce a regular VNHC of order k, we would like to determine the dynamics on the constraint manifold Γ. Intuitively, these dynamics should be parameterized by (q_u, p_u) since q_a is a function of these as specified by $h(q, p_u) = 0$. Unfortunately, $\dot{q}_u$ depends on p_a, and for general systems one cannot solve explicitly for p_a in terms of (q_u, p_u). This is because the $\dot{p}$ dynamics contains the coupling term $(I_n \otimes p^{\mathsf{T}})\nabla_{q_u} M(q)p$.

We now introduce an assumption so we can solve explicitly for the constrained dynamics.

Assumption 4. The Hamiltonian system has an inertia matrix that does not depend on the unactuated coordinates:

$$\nabla_{q_u} M(q) = \mathbf{0}_{n(n-k)\times n}.$$

Theorem 2.11. *Let $\mathscr{H}$ be a mechanical system in simply actuated coordinates satisfying Assumption 4. Let $h(q, p_u) = 0$ be a regular VNHC of order k with constraint manifold Γ. Suppose that on Γ one can solve for q_a as a function $q_a = f(q_u, p_u)$. Then the constrained dynamics are given by*

$$\left.\begin{aligned}\dot{q}_u &= \begin{bmatrix} I_{(n-k)} & \mathbf{0}_{(n-k)\times k} \end{bmatrix} M^{-1}(q)p \\ \dot{p}_u &= -\nabla_{q_u} V(q)\end{aligned}\right|_{\substack{q_a = f(q_u, p_u) \\ p_a = g(q_u, p_u)}},\tag{2.14}$$

where

$$g(q_u, p_u) :=$$
$$\left(dh_q M^{-1}(q)\begin{bmatrix} \mathbf{0}_{(n-k)\times k} \\ I_k \end{bmatrix}\right)^{-1}\left(dh_{p_u}\nabla_{q_u} V(q) - dh_q M^{-1}(q)\begin{bmatrix} I_{n-k} \\ \mathbf{0}_{k\times(n-k)} \end{bmatrix} p_u\right)\Bigg|_{q_a=f(q_u,p_u)}.$$
$$(2.15)$$

---

[2]Under additional mild conditions [19]

Proof. Setting $e = h(q, p_u)$ and using the fact that $\nabla_{q_u} M^{-1}(q) = 0$, we find that

$$\dot{e} = dh_q M^{-1}(q)p - dh_{p_u} \nabla_{q_u} V(q).$$

Observe that

$$dh_q M^{-1}(q)p = dh_q M^{-1}(q) \begin{bmatrix} p_u \\ p_a \end{bmatrix}$$

$$= dh_q M^{-1}(q) \begin{bmatrix} I_{n-k} & \mathbf{0}_{(n-k)\times k} \\ \mathbf{0}_{k\times(n-k)} & I_k \end{bmatrix} \begin{bmatrix} p_u \\ p_a \end{bmatrix}$$

$$= dh_q M^{-1}(q) \begin{bmatrix} I_{n-k} \\ \mathbf{0}_{k\times(n-k)} \end{bmatrix} p_u + dh_q M^{-1}(q) \begin{bmatrix} \mathbf{0}_{(n-k)\times k} \\ I_k \end{bmatrix} p_a.$$

On the constraint manifold, we have $e = \dot{e} = 0$, which means

$$dh_q M^{-1}(q) \begin{bmatrix} \mathbf{0}_{(n-k)\times k} \\ I_k \end{bmatrix} p_a = dh_{p_u} \nabla_{q_u} V(q) - dh_q M^{-1}(q) \begin{bmatrix} I_{n-k} \\ \mathbf{0}_{k\times(n-k)} \end{bmatrix} p_u.$$

Since h is regular and $\nabla_{q_u} M^{-1}(q) = 0$, we have that

$$\text{rank}\left(dh_q M^{-1}(q) \begin{bmatrix} \mathbf{0}_{(n-k)\times k} \\ I_k \end{bmatrix} \right) = k.$$

Solving for p_a gives

$$p_a(q, p_u) = \left(dh_q M^{-1}(q) \begin{bmatrix} \mathbf{0}_{(n-k)\times k} \\ I_k \end{bmatrix} \right)^{-1} \left(dh_{p_u} \nabla_{q_u} V(q) - dh_q M^{-1}(q) \begin{bmatrix} I_{n-k} \\ \mathbf{0}_{k\times(n-k)} \end{bmatrix} p_u \right).$$

This yields a function $p_a(q, p_u)$. However, on Γ we have $q_a = f(q_u, p_u)$, which we use to solve for $p_a = g(q_u, p_u)$. Since q_a and p_a can be computed directly from (q_u, p_u), the dynamics on Γ are parameterized only by $(\dot{q}_u, \dot{p}_u)$. $\qquad\square$

Theorem 2.11 shows that, for a particular class of systems and constraints, the dynamics on Γ are entirely described by the $2(n - k)$ unactuated coordinates. This is true regardless of the number of degrees of freedom of the system.

The following corolllay applies Theorem 2.11 to systems with only one unactuated coordinate.

Corollary. *Let $\mathcal{H}$ be the system (2.10) with degree of underactuation one. Suppose $\mathcal{H}$ satisfies*

Assumption 4. Let $h(q, p_u) = 0$ be a regular VNHC of order $(n - 1)$ of the form $h(q, p_u) = q_a - f(q_u, p_u)$, where f is a suitably defined C^2 function. Then $dh_q = \begin{bmatrix} -\partial_{q_u} f & I_{(n-1)} \end{bmatrix}$. Defining $e_1 := (1, 0, \ldots, 0) \in \mathbb{R}^n$, the actuated momentum is

$$p_a = -\left(dh_q M^{-1}(q) \begin{bmatrix} \mathbf{0}_{1 \times (n-1)} \\ I_{(n-1)} \end{bmatrix} \right)^{-1} \left(\partial_{p_u} f \partial_{q_u} V + dh_q M^{-1}(q) e_1 p_u \right) \Bigg|_{q_a = f(q_u, p_u)} . \tag{2.16}$$

Since $q_u \in [\mathbb{R}]_{T_u}$ for some $T_u \in\ ]0, \infty]$ and $p_u \in \mathbb{R}$, the orbit $(q_u(t), p_u(t))$ traces out a curve on the 2D-plane $[\mathbb{R}]_{T_u} \times \mathbb{R}$ which we call the (q, p)-plane.

2.4 Summary of Results

In this chapter, we developed the framework of virtual nonholonomic constraints for underactuated Hamiltonian mechanical systems. We made the following assumptions:

1. The input matrix $B(q) \equiv B \in \mathbb{R}^{n \times k}$ is constant and full rank.

2. The input matrix has a left-annihilator $B^\perp \in \mathbb{R}^{(n-k) \times n}$.

3. The annihilator matrix $B^\perp$ is right semi-orthogonal.

These assumptions allowed us to define a canonical change of coordinates into the simply actuated coordinates $(q, p) \in \mathcal{Q} \times \mathcal{P}$, where $q = (q_u, q_a)$ and $p = (p_u, p_a)$.

We defined a virtual nonholonomic constraint as a function $h \in C^2(\mathcal{Q} \times \mathcal{P}; \mathbb{R}^k)$ which has no singular points on its constraint manifold

$$\Gamma = \left\{ (q, p) \mid h(q, p) = 0, dh_q \dot{q} + dh_p \dot{p} = 0 \right\}.$$

We then showed that a VNHC $h : \mathcal{Q} \times \mathcal{P}_u \to \mathbb{R}^k$ is regular if and only if the square matrix

$$\left(dh_q M^{-1}(q) - dh_{p_u}(I_{n-k} \otimes p^\top) \nabla_{q_u} M^{-1}(q) \right) \begin{bmatrix} \mathbf{0}_{(n-k) \times k} \\ I_k \end{bmatrix}$$

is invertible on Γ.

To find the explicit equations for constrained dynamics of a regular VNHC, we made the following assumptions:

- The inertia matrix satisfies $\nabla_{q_u} M(q) = \mathbf{0}_{n(n-k) \times n}$.

- On Γ, one can solve for q_a as a function of (q_u, p_u).

If these assumptions hold, one can solve for $p_a = g(q_u, p_u)$ on Γ. The constrained dynamics are then given by $(\dot{q}_u, \dot{p}_u)$ subject to $h(q, p_u) = 0$ and $p_a = g(q_u, p_u)$.

Finally, we saw the benefit of using VNHCs is that they reduce the dimensionality of the system from $2n$ equations of motion to $2(n - k)$ equations, which significantly reduces the complexity of analyzing large systems. In particular, if the system has degree of underactuation one, the dynamics reduce to a 2D system on the "(q, p)-plane" $[\mathbb{R}]_T \times \mathbb{R}$.

Chapter 3

Application of VNHCS: The Variable Length Pendulum

3.1   Motivation

The variable length pendulum (VLP) is a classical underactuated dynamical system which is often used to model the motion of a person on a swing [8, 16]. The VLP also represents the motion of the load at the end of a crane, the (simplified) motion of a gymnast on a bar [15], and the tuned-mass-damper systems which stabilize skyscrapers [41].

The motion of the VLP has been well studied (see for instance [39]), and many control mechanisms exist to stabilize trajectories of the system. While many of these controllers are time-dependent, Xin and Liu [20] offer a time-independent technique to inject energy into the VLP. They design a controller through a technique called *energy shaping* and prove that it stabilizes any desired energy level set. However, their control input depends on a pre-specified target energy and requires knowledge of the current total energy of the VLP. This makes their energy injection mechanism "ad-hoc" in the sense that it is tailored very specifically to the VLP, and is not generalizable to a larger methodology.

It may be better to base the control design on natural biological behaviour. In this chapter we will make use of the general VNHC framework developed in Chapter 2 to add and remove energy from the VLP in a time-independent manner. We'll show that, unlike energy shaping, VNHCs can be used to stabilize energy levels while maintaining the structured motion of a human on a swing.
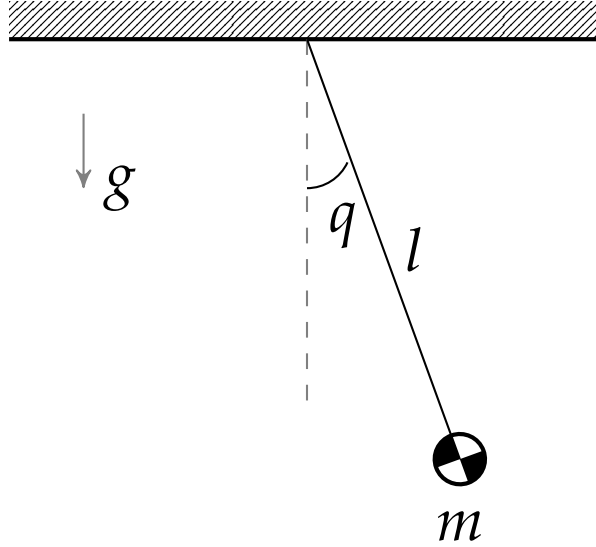
FIGURE 3.1: The variable length pendulum is a mass attached to the tip of a massless rod which can change length.

3.2   Dynamics of the Variable Length Pendulum

We will model the VLP as a point mass m connected to a fixed pivot by a massless rod of varying length l with angle $q \in \mathbb{S}^1$ from the vertical, as in Figure 3.1. We will ignore any damping and frictional forces in this model. In a realistic VLP, the rod length l varies between some minimum length $\underline{l} \geq 0$ and some maximum length $\bar{l} > \underline{l}$. The configuration of the VLP is the vector $\mathbf{q} := (q, l) \in \mathbb{S}^1 \times [\underline{l}, \bar{l}]$.

Using this configuration, we will compute the Hamiltonian dynamics of the system. The cartesian position of the mass at the tip of the pendulum is given by $x = (l\sin(q), -l\cos(q))$, while its velocity is $\dot{x} = (\dot{l}\sin(q) + l\cos(q)\dot{q}, -\dot{l}\cos(q) + l\sin(q)\dot{q})$. Computing the kinetic energy T yields

$$T(\mathbf{q}, \dot{\mathbf{q}}) = \frac{1}{2}m\|\dot{x}\|^2 = \frac{1}{2}m\left(\dot{l}^2 + l^2\dot{q}^2\right).$$

The potential energy P with respect to the pivot (under a gravitational acceleration g) is

$$P(\mathbf{q}) = -mgl\cos(q).$$

Collecting the kinetic energy into a quadratic form, we get the Lagrangian

$$\mathscr{L}(\mathbf{q}, \dot{\mathbf{q}}) = \frac{1}{2}\dot{\mathbf{q}}^\mathsf{T} D(\mathbf{q})\dot{\mathbf{q}} - P(\mathbf{q}) = \frac{1}{2}\begin{bmatrix} \dot{q} & \dot{l} \end{bmatrix}\begin{bmatrix} ml^2 & 0 \\ 0 & m \end{bmatrix}\begin{bmatrix} \dot{q} \\ \dot{l} \end{bmatrix} + mgl\cos(q).$$

Computing the conjugate of momenta to $\mathbf{q}$, we get

$$\mathbf{p} := \begin{bmatrix} p \\ p_l \end{bmatrix} = \begin{bmatrix} ml^2 \dot{q} \\ m\dot{l} \end{bmatrix}.$$

Performing the Legendre transform on $\mathscr{L}$ and setting $M(\mathbf{q}) := D(\mathbf{q})$, $V(\mathbf{q}) := P(\mathbf{q})$, we get the Hamiltonian (2.11) whose dynamics (2.12) resolve to

$$\mathscr{H} = \frac{1}{2} \begin{bmatrix} p & p_l \end{bmatrix} \begin{bmatrix} \frac{1}{ml^2} & 0 \\ 0 & \frac{1}{m} \end{bmatrix} \begin{bmatrix} p \\ p_l \end{bmatrix} - mgl\cos(q), \tag{3.1}$$

$$\begin{cases} \dot{q} = \frac{p}{ml^2} \\ \dot{l} = \frac{p_l}{m} \\ \dot{p} = -mgl\sin(q) \\ \dot{p_l} = \frac{p^2}{ml^3} + mg\cos(q) + \tau. \end{cases}$$

The control input is a force $\tau \in \mathbb{R}$ affecting the dynamics of p_l, acting colinearly with the rod. We assume the force does not affect the dynamics of p in any way - that is, the control input cannot enact any lateral force on the pendulum. This makes the VLP into an underactuated mechanical system with degree of underactuation one. It is also a useful assumption because it means $(\mathbf{q}, \mathbf{p})$ are simply actuated coordinates, which allows us to apply the theory of VNHCs we developed in Chapter 2.

Let us define the VNHC $l = L(q, p)$, by which we mean we are actually defining the VNHC $h(\mathbf{q}, \mathbf{p}) = l - L(q, p) = 0$ of order 1. The VLP satisfies $\nabla_q M^{-1}(\mathbf{q}) = \mathbf{0}_{2 \times 2}$. By Theorem 2.10, $h(\mathbf{q}, \mathbf{p})$ is a regular VNHC whenever $L(q, p)$ is C^2 because

$$dh_{\mathbf{q}} M^{-1}(\mathbf{q}) B = \begin{bmatrix} -\frac{\partial L}{\partial q} & 1 \end{bmatrix} \begin{bmatrix} \frac{1}{ml^2} & 0 \\ 0 & \frac{1}{m} \end{bmatrix} \begin{bmatrix} 0 \\ 1 \end{bmatrix} = \frac{1}{m}$$

is always full rank. The constraint manifold is $\Gamma = \mathbb{S}^1 \times \mathbb{R}$, which is parameterized by the unactuated phase (q, p). By Theorem 2.11, the constrained dynamics are described entirely by $(\dot{q}, \dot{p})$ with l replaced by $L(q, p)$:

$$\begin{cases} \dot{q} = \frac{p}{mL^2} \\ \dot{p} = -mgL\sin(q). \end{cases} \tag{3.2}$$

Note that we suppress the function notation of $L(q, p)$ for clarity.

The total mechanical energy of the system restricted to the constraint manifold is

(a) A person standing on a swing has their center of mass close to the pivot.

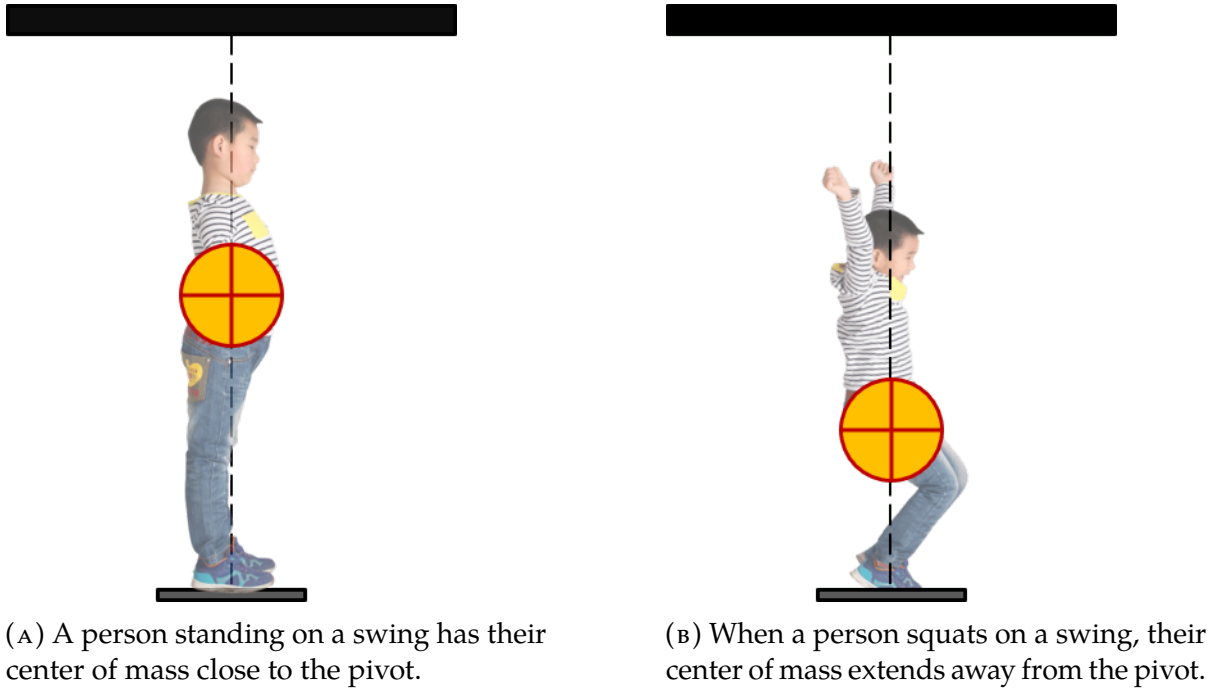(b) When a person squats on a swing, their center of mass extends away from the pivot.

Figure 3.2: The VLP representation of a person on a standing swing.

given by (3.3), where $L(q, p)$ and $\dot{L}(q, p)$ are known.

$$E(q, p) = \frac{1}{2} \frac{p^2}{mL^2} + \frac{1}{2} \dot{L}^2 - mgL \cos(q). \tag{3.3}$$

In the rest of this chapter, we will derive a C^2 function $L(q, p)$ based on natural human motion. This function will produce constrained dynamics that inject energy into the VLP.

3.3   The VLP Constraint

To motivate why a VNHC could inject energy into the VLP in a human-like manner, we will examine a person standing on a swing. As can be seen in Figure 3.2, a person's center of mass moves closer to the swing's pivot when they stand, and moves away from the pivot when they squat. This is equivalent to the VLP model from Figure 3.1, where standing and squatting correspond to shortening and lengthening the pendulum respectively.

The action of regulating pendulum length to inject energy into the VLP is known as "pumping". Piccoli and Kulkarni [16] asked whether the pumping strategy performed by children is time-optimal, assuming the children could squat or stand instantaneously.

Indeed, they discovered that children increase the height of their swing as fast as is physically possible.

A child's optimal pumping strategy is the following: they stand at the lowest point of the swing, and squat at the highest point. Looking at the VLP representation, the pendulum shortens at the bottom of the swing, and lengthens at the top. For an intuitive explanation, conservation of angular momentum indicates that shortening the pendulum at the bottom forces the mass to gain speed to compensate for the reduced length [8]. Energy is not conserved in this process, so the pendulum gains kinetic energy and reaches a higher point at the peak of its swing. Lengthening the pendulum when it reaches this peak means gravity imparts a larger angular momentum to the mass by the time it reaches the bottom of its swing, which in turn is converted to a higher velocity when the pendulum is shortened. By alternating these processes, the pendulum experiences an average net gain in rotational energy.

Notice that the child's pumping strategy requires knowledge of when the system is at the "bottom" or "top" of the swing. Since being at the bottom is equivalent to having angle $q = 0$ and being at the top is equivalent to having momentum $p = 0$, a controller based on this strategy will necessarily involve the full unactuated phase (q, p). This is why we must use VNHCs instead of other methods (such as VHCs) to perform this maneuver.

The time-optimal controller from [16] is, in our notation,

$$L^\star(q, p) := -\,\text{sgn}\,(qp)\,,$$

which is a piecewise-continuous controller that varies between ± 1. We could set our constraint to be $l = L^\star(q, p)$, but this is not a VNHC because it is not C^2. Additionally, it would force us to assume that $l \in \{-1, 0, 1\}$ and that one can switch l instantaneously. Since we need to enforce the constraint using the physical input τ (which would ideally emulate realistic human motion), we cannot use $L^\star$ as our VNHC. We will instead find an alternate representation of $L^\star$ which can be converted into a VNHC, and which allows $l \in [\underline{l}, \bar{l}]$.

Figure 3.3a displays $L^\star(q, p)$ on the (q, p)-plane. Note that the length remains constant inside each quadrant and changes only when it crosses one of the axes. Using this fact, we can redefine the time-optimal pumping strategy as a function of $\theta := \arctan_2(p, q)$. Abusing notation, we denote this by $L^\star(\theta)$, which is defined in (3.4). Figure 3.3b shows

(A) The time-optimal controller $L^\star(q, p)$ mapped onto the (q, p)-plane. Here, red corresponds to $L^\star(q, p) = -1$ and blue to $L^\star(q, p) = 1$.

(B) The time-optimal controller converted to the alternate representation $L^\star(\theta)$.
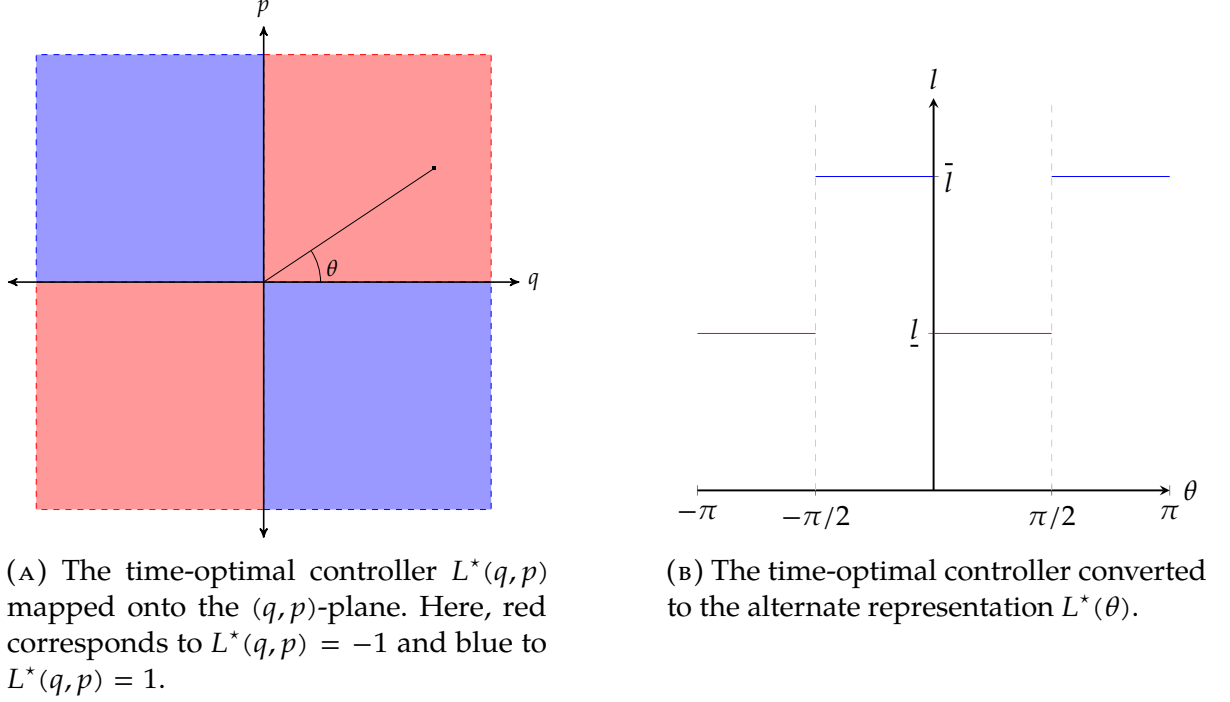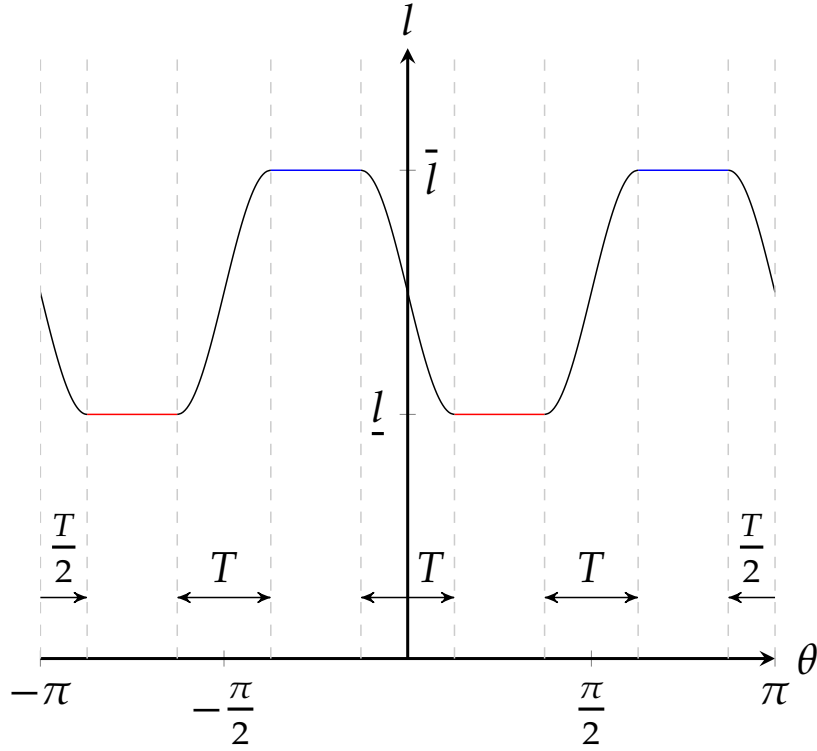
FIGURE 3.3: The time-optimal controller for a standing swing as derived by [16]. The colour red corresponds to standing, blue to squatting, and $\theta := \arctan_2(p, q)$ is the angle of the VLP phase in the (q, p)-plane.

the graph of $L^\star(\theta)$, where now the length varies between $[\underline{l}, \bar{l}]$ rather than $\{-1, 0, 1\}$.

$$L^\star(\theta) := \begin{cases} \bar{l} & \theta \in [-\frac{\pi}{2}, 0[\cup [\frac{\pi}{2}, \pi[\\ \underline{l} & \theta \in [-pi, -\frac{\pi}{2}[\cup [0, \frac{\pi}{2}[. \end{cases} \tag{3.4}$$

We now define a continuous function which approximates $L^\star(\theta)$. Let $\Delta l := (\bar{l} - \underline{l})/2$ and $l_{\text{avg}} := (\bar{l} + \underline{l})/2$. Let $T \in]0, \frac{\pi}{2}]$ be a parameter of our choosing. By intelligently attaching sinusoids of frequency $\omega = \frac{\pi}{T}$ to $L^\star(\theta)$ (see Figure 3.4), we get a family of C^1 constraints $L_T(\theta)$ parameterized by T:

$$L_T(\theta) := \begin{cases} \bar{l} & \theta \in \left[-\frac{\pi}{2} + \frac{T}{2}, -\frac{T}{2}\right] \cup \left[\frac{\pi}{2} + \frac{T}{2}, \pi - \frac{T}{2}\right] \\ \underline{l} & \theta \in \left[-\pi + \frac{T}{2}, -\frac{\pi}{2} - \frac{T}{2}\right] \cup \left[\frac{T}{2}, \frac{\pi}{2} - \frac{T}{2}\right] \\ -\Delta l \sin(\omega(\theta + \pi)) + l_{\text{avg}} & \theta \in \left[-\pi, -\pi + \frac{T}{2}\right] \\ -\Delta l \sin(\omega\theta) + l_{\text{avg}} & \theta \in [-\frac{T}{2}, \frac{T}{2}] \\ \Delta l \sin(\omega(\theta - a)) + l_{\text{avg}} & \theta \in \left[a - \frac{T}{2}, a + \frac{T}{2}\right] \text{ for } a \in \left\{-\frac{\pi}{2}, \frac{\pi}{2}\right\} \\ -\Delta l \sin(\omega(\theta - \pi)) & \theta \in \left[\pi - \frac{T}{2}, \pi\right]. \end{cases} \tag{3.5}$$

FIGURE 3.4: The continuous VLP constraint $l = L_T(\theta)$.

This family of constraints approximates $L^\star(\theta)$ because

$$\lim_{T \to 0} L_T(\theta) = L^\star(\theta).$$

Unfortunately, while $L_T(\theta)$ is continuously-differentiable, it is not twice-differentiable for most values of T. If we wish to use it as a VNHC, we must ensure that either the generalized forces τ acting on p_l can be discontinuous (which is certainly achievable by humans), or we must find a value of T where this constraint is at least C^2. Thankfully, setting $T = \frac{\pi}{2}$ yields the smooth function $L_{\frac{\pi}{2}}(\theta)$, which can be simplified from (3.5) into
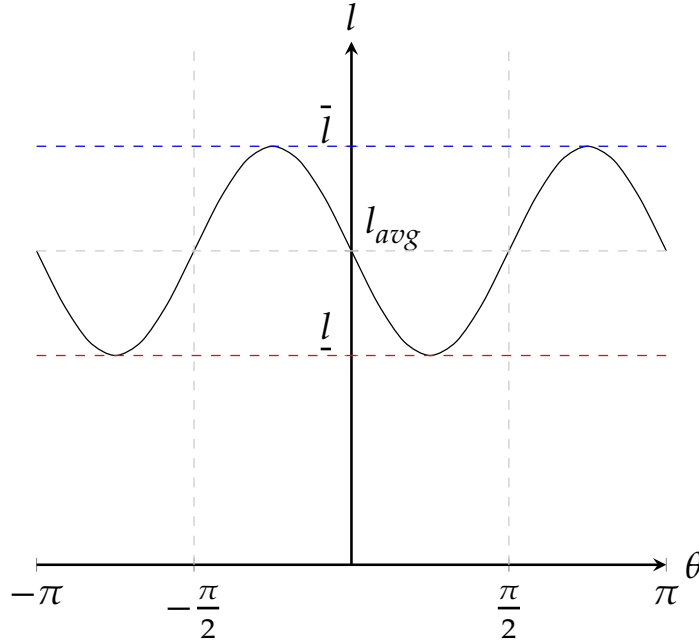
$$L_{\frac{\pi}{2}}(\theta) = -\Delta l \sin(2\theta) + l_{\text{avg}}. \tag{3.6}$$

This smooth constraint is plotted for demonstration in Figure 3.5.

Because $L_{\frac{\pi}{2}}(\theta)$ is smooth and it approximates $L^\star(\theta)$, we set our VNHC to be

$$h(\mathbf{q}, \mathbf{p}) = l - L_{\frac{\pi}{2}}\left(\theta(q, p)\right).$$

Before proving the VLP will gain energy under this VNHC, we must rigorously

FIGURE 3.5: The smoothed VLP constraint $l = L_{\frac{\pi}{2}}(\theta)$.

define what that means. If any initial condition of the constrained dynamics converges to the point $(q, p) = (0, 0)$, the momentum must be decreasing over time, so the VLP will clearly be losing energy. A notion of energy injection must therefore require that the origin repels all solutions. We need to avoid closed orbits or limit cycles in the (q, p)-plane, so that the system can always reach higher speeds. Finally, we want the VLP's momentum to increase on average, regardless of its initial value. This intuition is captured mathematically by the following definition.

Definition 3.1. Let $D \subset \mathbb{R}^2$ be open with $0 \in D$. Let $f : D \rightarrow \mathbb{R}^2$ be locally Lipschitz with $f(0) = 0$. The system described by $\dot{x} = f(x)$ *gains energy on D* if

1. The origin is a repeller (or equivalently, the origin is asymptotically stable in negative time).

2. For all compact sets $K \subset D$ and for almost every initial condition $x(0) \in K$, there exists $T > 0$ such that $x(t) \notin K$ ($\forall t > T$).

The system *loses energy on D* if it gains energy in negative-time.

The second property of Definition 3.1 allows the system to have unstable equilibria, but not limit cycles nor closed orbits. The next definition ties this notion of energy gain to VNHCs.

Definition 3.2. A regular VNHC $h(\mathbf{q}, \mathbf{p}) = 0$ *injects (dissipates) energy* if the constrained dynamics gain (lose) energy everywhere on the constraint manifold, except possibly on a set of measure zero.

We can now prove our VNHC injects energy into the VLP. As part of the proof, we will require the following lemma.

Lemma 3.3. *For any $x, y \in \mathbb{R}$,*

$$\text{sgn}\left(x^3 - y^3\right) = \text{sgn}\left(x - y\right).$$

Proof. Observe that $x^3 - y^3 = (x - y)(x^2 + xy + y^2)$. The inequality $x^2 + xy + y^2 \geq 0$ holds because

$$x^2 + xy + y^2 = \left(x + \frac{y}{2}\right)^2 + \frac{3y^2}{4} \geq 0,$$

which proves the lemma. □

We will show that the constrained dynamics trace out a curve on the (q, p)-plane which is diverging from the origin. This implies that the momentum p is increasing in magnitude whenever the curve hits the p-axis, which in turn means the VLP is gaining energy on average.

Theorem 3.4. *Define $\theta := \arctan_2(p, q)$. Let $L : \mathbb{S}^1 \to [\underline{l}, \bar{l}]$ be a C^2 function of θ. A regular VNHC of the form $h(\mathbf{q}, \mathbf{p}) = l - L(\theta)$ injects energy into the VLP if there exists $l_{avg} \in [\underline{l}, \bar{l}]$ such that*

$$\left(l_{avg} - L(\theta)\right) \sin(2\theta) \geq 0 \ \forall \theta \in \mathbb{S}^1, \tag{3.7}$$

with the property that the inequality is strict except at the coordinate axes. If the inequality is flipped, the VNHC dissipates energy.

Proof. The constraint manifold for h is the cylinder $\Gamma = \mathbb{S}^1 \times \mathbb{R}$. In negative-time, the dynamics on Γ are

$$f(q, p) = -\begin{bmatrix} \dot{q} \\ \dot{p} \end{bmatrix} = \begin{bmatrix} -\frac{p}{mL(\theta)^2} \\ mgL(\theta) \sin(q) \end{bmatrix}. \tag{3.8}$$

Because $q \in \mathbb{S}^1$, the only equilibria of these dynamics are at $(q, p) = (0, 0)$ and $(q, p) = (\pi, 0)$. To prove the origin of the positive-time system (3.2) is a repeller, we will show the origin of the negative-time system (3.8) is almost everywhere globally asymptotically stable.

Choose, as a candidate Lyapunov function, the energy for the average-length pendulum with zero-potential at the bottom of the swing:

$$E_{\text{avg}}(q, p) := \frac{1}{2} \frac{p^2}{ml_{\text{avg}}^2} + mgl_{\text{avg}}(1 - \cos(q)).$$

This is positive definite at $(0, 0)$ and has compact sublevel sets on Γ. The derivative of E_{avg} along (3.2) is

$$\dot{E}_{\text{avg}}^+ = -\frac{g \sin(q)p \left(L(\theta)^3 - l_{\text{avg}}^3\right)}{l_{\text{avg}}^2 L(\theta)^2}, \tag{3.9}$$

and the derivative of E_{avg} along (3.8) is

$$\dot{E}_{\text{avg}}^- = -\dot{E}_{\text{avg}}^+. \tag{3.10}$$

The sign of $\sin(q)p$ depends only on the quadrant in the (q, p)-plane. In fact, it is easy to show that

$$\text{sgn}\left(\sin(q)p\right) = \text{sgn}\left(\sin(2\theta)\right).$$

Furthermore, by Lemma 3.3 we have

$$\text{sgn}\left(L(\theta)^3 - l_{\text{avg}}^3\right) = \text{sgn}\left(L(\theta) - l_{\text{avg}}\right).$$

The positive-time derivative (3.9) is nonnegative since

$$\begin{aligned}
\text{sgn}\left(\dot{E}_{\text{avg}}^+\right) &= \text{sgn}\left(-\sin(q)p\left(L(\theta)^3 - l_{\text{avg}}^3\right)\right) \\
&= \text{sgn}\left(-\sin(2\theta)\left(L(\theta) - l_{\text{avg}}\right)\right) \\
&= \text{sgn}\left((l_{\text{avg}} - L(\theta))\sin(2\theta)\right) \\
&\geq 0 \text{ (by assumption).} \tag{3.11}
\end{aligned}$$

Using (3.10) and (3.11) we can determine that $\text{sgn}\left(\dot{E}_{\text{avg}}^-\right) \leq 0$. Thus, E_{avg} is a Lyapunov function for (3.8), which means the negative-time system is stable [42].

Let us briefly analyze the upright equilibrium. Label the set of initial conditions converging to $(\pi, 0)$ in positive time by

$$\Pi_0^+ := \left\{(q_0, p_0) \in \Gamma \mid \lim_{t \to \infty}(q(t), p(t)) = (\pi, 0)\right\},$$

and the set of initial conditions converging to $(\pi, 0)$ in negative time by Π_0^-. Take now

the sublevel set

$$E_{(\pi,0)} := \left\{ (q,p) \in \Gamma \mid E_{\mathrm{avg}}(q,p) \leq E_{\mathrm{avg}}(\pi,0) \right\}.$$

From (3.11), all sublevel sets of E_{avg} are negatively invariant in positive-time, which means complements of sublevel sets are positively invariant. Hence, the system cannot possibly converge to $(\pi,0)$ if it is initialized on $\left(E_{(\pi,0)} \right)^C = \Gamma \backslash E_{(\pi,0)}$. This implies that $\Pi_0^+ \subset E_{(\pi,0)}$. Similarly, the interior of $E_{(\pi,0)}$ is positively invariant for (3.8), which implies $\Pi_0^- \subset \left(E_{(\pi,0)} \right)^C \cup (\pi,0)$.

The linearization of (3.2) at $(\pi,0)$ is given by

$$\begin{bmatrix} 0 & \frac{1}{mL(0)^2} \\ mgL(0) & 0 \end{bmatrix}, \tag{3.12}$$

which has eigenvalues at $\lambda = \pm\sqrt{\frac{g}{L(0)}}$. Linearizing (3.8) at this point yields the same eigenvalues. Since one eigenvalue of (3.12) is positive and one is negative, the stable manifold theorem tells us that both Π_0^+ and Π_0^- are one-dimensional [53]. This implies the origin cannot be globally asymptotically stable for (3.8); however, we can still show it is asymptotically stable for almost every initial condition because Π_0^+ and Π_0^- are of measure zero within Γ.

We cannot linearize (3.2) at $(0,0)$ to prove the origin is a repeller, because $\theta(0,0)$ is not well-defined. Instead, let $D := \Gamma \backslash \Pi_0^-$. We will prove that (3.8) asymptotically converges to $(0,0)$ if it is initialized on D. First, define the zero-set

$$Z = \left\{ (q,p) \in \Gamma \mid \dot{E}_{\mathrm{avg}}(q,p) = 0 \right\}.$$

It is easy to show that Z is the union of the coordinate axes

$$Z = \mathbb{S}^1 \times \{0\} \cup \{0\} \times \mathbb{R}.$$

Krasovskii-LaSalle tells us that solutions to (3.8) converge to the largest invariant set in $Z \cap D$ [50]. Since $f(q,p) = (0,0)$ on D only when $(q,p) = (0,0)$, the origin is asymptotically stable on D for the negative-time system. In particular, the origin is asymptotically stable for every initial condition in the interior of $E_{(\pi,0)}$. Hence, the positive-time system is diverging away from the origin in the (q,p) plane, which means the origin is a repeller.

We now prove the system escapes compact sets in finite time. Let $x(t) = (q(t),p(t))$ be the orbit for the positive-time system. Let $K \subset \Gamma$ be compact and assume $x(0) \in K \backslash \left(\Pi_0^+ \cup \{(0,0)\} \right)$. For a proof by contradiction, suppose that for all $T > 0$ there exists

$t' > T$ where $x(t') \in K$. Let

$$k := \max_{(q,p) \in K} E_{avg}(q,p),$$

be the largest energy value attained in K, and let E_k be its sublevel set.

Since E_k contains K and $x(t') \in K$, it follows that $x(t') \in E_k$. Furthermore, negative invariance of E_k means the half orbit $x([0, t'])$ is contained fully within E_k. In particular, $x(T) \in E_k$. However, T was chosen arbitrarily, which implies $x(t) \in E_k$ for all $t \in [0, \infty[$. Since E_k is compact, $x(t)$ has a positive limit set in E_k which, by Poincaré-Bendixson, is either an equilibrium or a closed orbit [52]. We will show this positive limit set must be an equilibrium and thereby reach our contradiction.

Suppose the system had a closed orbit. The orbit would necessarily be contained in a level set of E_{avg}, since this is a non-decreasing function and closed orbits are periodic. Thus, E_{avg} is constant along the orbit, which means the orbit is an invariant subset of the set Z consisting of the two axes. However, the only invariant subsets of Z are equilibria, so the system cannot contain closed orbits.

The lack of closed orbits means the positive limit set of $x(t)$ must be one of the equilibria. The origin is a repeller and $x(0) \neq (0,0)$, which means $x(t)$ is converging to $(\pi, 0)$. This is a contradiction, since we assumed $x(0) \notin \Pi_0^+$.

We conclude that the VNHC is injecting energy into the VLP. By flipping the inequality of (3.7) we find the VLP is gaining energy in negative-time, so the VNHC is dissipating energy. $\qquad\square$

Corollary. *Recall that*

$$L_{\frac{\pi}{2}}(\theta) := -\Delta l \sin(2\theta) + l_{avg},$$

and define

$$L_{\frac{\pi}{2}}^-(\theta) := \Delta l \sin(2\theta) + l_{avg}.$$

The VNHC $l = L_{\frac{\pi}{2}}(\theta)$ *injects energy into the VLP, while* $l = L_{\frac{\pi}{2}}^-(\theta)$ *dissipates energy.*

Proof. Both VNHCs satisfy Theorem 3.4 because

$$\left(l_{avg} - L_{\frac{\pi}{2}}(\theta) \right) \sin(2\theta) = \Delta l \sin^2(2\theta) \geq 0,$$

and

$$\left(l_{avg} - L_{\frac{\pi}{2}}^-(\theta) \right) \sin(2\theta) = -\Delta l \sin^2(2\theta) \leq 0,$$

where the inequalities are strict everywhere except the coordinate axes. $\qquad\square$

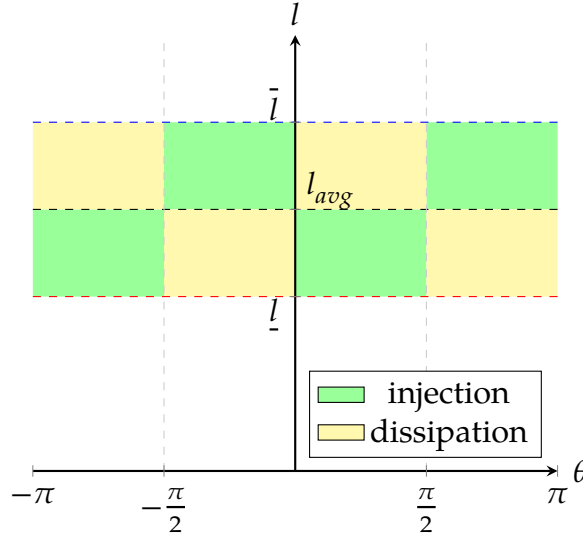The class of VNHCs which satisfies Theorem 3.4 is illustrated graphically in Figure

FIGURE 3.6: Any VNHC of the form $l = L(\theta)$ where $L(\theta)$ is entirely contained within the green (yellow) regions will inject (dissipate) energy.

3.6. To stabilize specific energy level sets, one simple approach is to switch between injection and dissipation VNHCs when the momentum p reaches a pre-determined value at the bottom of the swing. For the VNHCs we designed in this chapter, this means toggling between $L_{\frac{\pi}{2}}(\theta)$ and $L_{\frac{\pi}{2}}^{-}(\theta)$, with some hysteresis to avoid infinite switching.

Theorem 3.4 provides an alternate explanation for why the optimal pumping strategy $L^{\star}(\theta)$ works so well at injecting energy: it maximizes the derivative of E_{avg} under the restriction $l \in [\underline{l}, \bar{l}]$, so that the orbit in the (q, p)-plane diverges from the origin as fast as possible.

Let us define $(L^{\star})^{-}(\theta)$ by swapping the order of $\underline{l}$ and $\bar{l}$ in $L^{\star}(\theta)$:

$$(L^{\star})^{-}(\theta) := \begin{cases} \underline{l} & \theta \in [-\frac{\pi}{2}, 0[\cup [\frac{\pi}{2}, \pi[\\ \bar{l} & \theta \in [-pi, -\frac{\pi}{2}[\cup [0, \frac{\pi}{2}[. \end{cases}$$

Since this function *minimizes* the derivative of E_{avg} under the restriction $l \in [\underline{l}, \bar{l}]$, one might predict that $(L^{\star})^{-}(\theta)$ is the optimal energy dissipation strategy for the VLP. This is, in fact, true. Piccoli and Kulkarni [16] showed that squatting at the lowest point of a swing and standing at the highest (instead of standing and squatting, respectively) produces the time-optimal trajectory for *stopping* a standing swing.

All together, the theory developed in this chapter shows that VNHCs can replicate the time-optimal pumping/dissipation strategies performed by humans on swings. Furthermore, we see that VNHCs are a powerful tool for creating simple energy stabi-

lization techniques based on natural human motion.

3.4   Simulation Results

Chapter 4

Application of VNHCs: The Acrobot

4.1 Motivation

The acrobot is a two-link pendulum, actuated at the center joint (as in Figure 4.1). Since its first description in 1990 [43], the acrobot has become a benchmark problem in control theory; it is an underactuated mechanical system which produces complex nonlinear motion from an easy-to-describe model. The acrobot models a gymnast on a bar, since it represents a torso (top link) and legs (bottom link) with motion generated by the swinging of the legs at the hips. It is also one of the simplest models for a biped walking robot [44].

Controlling the acrobot is a nontrivial task, since it is not feedback linearizable [43]. Several researchers have studied the swing-up problem of driving the acrobot to its equilibrium point above the bar using partial feedback linearization [45], energy-based control [17, 46], and through studying human motion [18, 47].

In gymnastics terminology, a "giant" is the motion a gymnast performs to achieve full rotations around the bar [48]. We are interested in using VNHCs to generate giant motion, with the aim of stabilizing desired energy levels. The control of giant motion for the acrobot has been studied in [5, 18], and some authors have used virtual holonomic constraints to achieve this behaviour [2, 3, 21]. However, these controllers are neither intuitive nor easy to design: [2] defines a constraint by inverting a trajectory in time onto the state space; [3] requires a cascade controller to stabilize both a constraint and a desired limit cycle in the state space; and [21] enforces the giant by adding an extra state to estimate velocity, which increases the dimensionality of the problem in a crude approach to using VNHCs.

In this chapter we will design a physically-intuitive VNHC which generates giant motion and prove the acrobot gains energy. In the process of completing this proof,
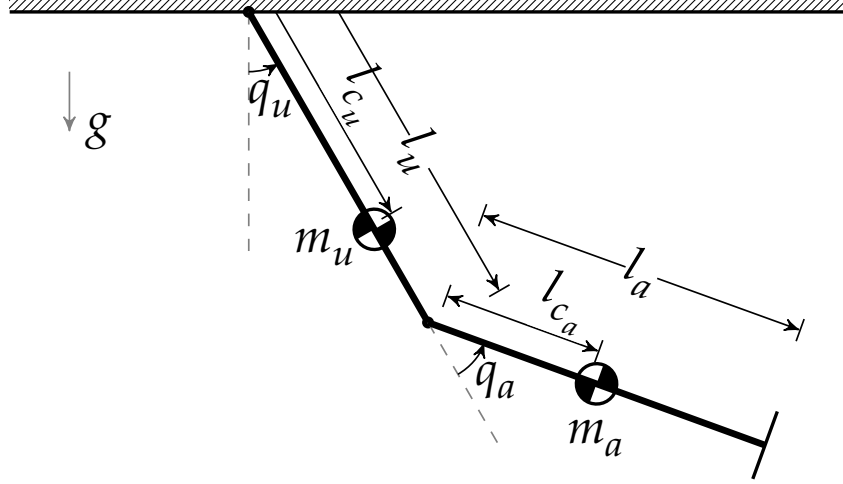
FIGURE 4.1: The general acrobot model, represented by two weighted rods differing in both length and mass.

we will arrive at a promising method which might one day be useful for generating energy-injecting VNHCs on arbitrary mechanical systems.

4.2 Dynamics of the Acrobot

Suppose we are given an acrobot as in Figure 4.1 modelling a gymnast hanging on a horizontal bar, where the "torso" has moment of inertia J_u and the "leg" has moment of inertia J_a (each with respect to their own center of mass). Let $q_u \in \mathbb{S}^1$ be the shoulder angle and $q_a \in \mathbb{S}^1$ be the hip angle, where only q_a is actuated. Collecting them together provides the configuration $q = (q_u, q_a) \in \mathbb{S}^1 \times \mathbb{S}^1$. The acrobot has inertia matrix D, potential function P (with respect to the horizontal bar), and input matrix B given as follows [21]:

$$D(q) = \begin{bmatrix} m_a l_u^2 + 2 m_a \cos(q_a) l_u l_{c_a} + m_a l_{c_a}^2 + m_u l_{c_u}^2 + J_u + J_a & m_a l_{c_a}^2 + m_a l_u l_{c_a} \cos(q_a) + J_a \\ m_a l_{c_a}^2 + m_a l_u l_{c_a} \cos(q_a) + J_a & m_a l_{c_a}^2 + J_a \end{bmatrix},$$

(4.1)

$$P(q) = g \left(m_a l_{c_a} (1 - \cos(q_u + q_a)) + (m_a l_u + m_u l_{c_u})(1 - \cos(q_u)) \right),$$

(4.2)

$$B(q) = \begin{bmatrix} 0 \\ 1 \end{bmatrix}.$$

(4.3)

While this is the most general representation of an acrobot, the dynamics become unwieldy. To make rigorous analysis of these dynamics more tractable, we begin by assuming the acrobot is comprised of two massless rods of equal length l, with equal
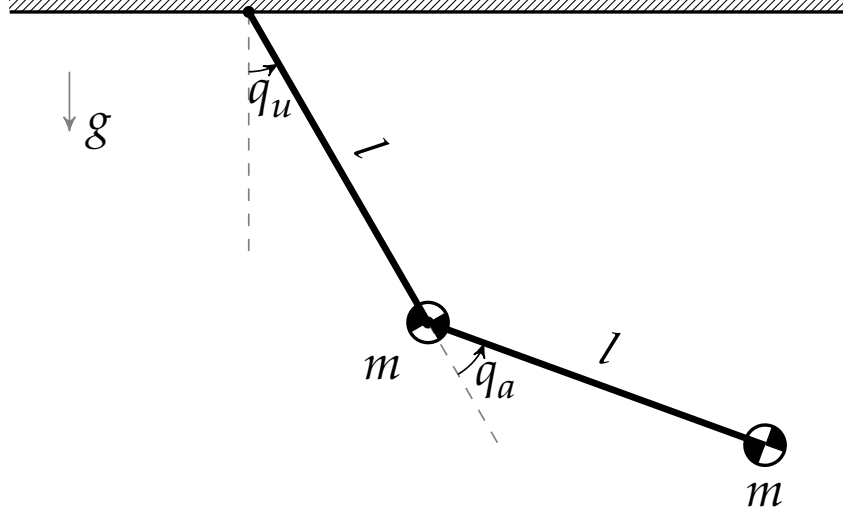
FIGURE 4.2: A simple acrobot has massless rods of equal length l and equal masses m at the tips.

point masses m at the tips. We call this a *simple* acrobot, which is displayed in Figure 4.2. We will also ignore any frictional forces at both the hip and shoulder joints. Finally, it is important to note that a real gymnast cannot swing their legs in full circles, though they are usually flexible enough to raise them parallel to the floor; for this reason, we assume that $q_a \in [-Q_a, Q_a]$ where $Q_a \in [\frac{\pi}{2}, \pi[$.

Since we are now working with a simple acrobot, we have $l_{c_u} = l_{c_a} = l_u = l_a = l$ and $m_u = m_a = m$. On top of this, the moments of inertia J_u and J_a of the rods vanish. Reducing (4.1-4.2) yields the simplified inertia matrix D_s and potential function P_s, where

$$D_s(q) = \begin{bmatrix} ml^2 \left(3 + 2\cos(q_a)\right) & ml^2 \left(1 + \cos(q_a)\right) \\ ml^2 \left(1 + \cos(q_a)\right) & ml^2 \end{bmatrix}, \tag{4.4}$$

$$P_s(q) = -mgl \left(2\cos(q_u) + \cos(q_u + q_a)\right). \tag{4.5}$$

Notation. For shorthand, we write $c_u := \cos(q_u)$, $c_a := \cos(q_a)$, and $c_{ua} := \cos(q_u + q_a)$. Likewise, $s_u := \sin(q_u)$, $s_a := \sin(q_a)$, and $s_{ua} := \sin(q_u + q_a)$.

Defining $M(q) := D_s(q)$ and $V(q) := P_s(q)$, we find the conjugate of momenta is

$p = (p_u, p_a) = M(q)\dot{q}$. The dynamics in (q, p) coordinates are given by

$$\mathscr{H}(q, p) = \frac{1}{2}p^{\mathsf{T}}M^{-1}(q)p - mgl\left(2c_u + c_{ua}\right), \tag{4.6}$$

$$\begin{cases} \dot{q} = M^{-1}(q)p \\ \dot{p}_u = -mgl\left(2s_u + s_{ua}\right) \\ \dot{p}_a = -\frac{1}{2}p^{\mathsf{T}}\nabla_{q_a}M^{-1}(q)p - mgls_{ua} + \tau, \end{cases}$$

where the inverse inertia matrix is

$$M^{-1}(q) = \frac{1}{ml^2\left(2 - c_a^2\right)}\begin{bmatrix} 1 & -\left(1 + c_a\right) \\ -\left(1 + c_a\right) & 3 + 2c_a \end{bmatrix}. \tag{4.7}$$

The control input is a force $\tau \in \mathbb{R}$ affecting only the dynamics of p_a, representing a torque acting on the hip joint. This means (q, p) are simply actuated coordinates inside the phase space $\mathcal{Q} \times \mathscr{P}$ where

$$\mathcal{Q} = \mathcal{Q}_u \times \mathcal{Q}_a := \mathbb{S}^1 \times \mathbb{S}^1,$$

and

$$\mathscr{P} = \mathscr{P}_u \times \mathscr{P}_a := \mathbb{R} \times \mathbb{R}.$$

This allows us once again to apply the theory of VNHCs from Chapter 2.

Let us define the VNHC $h(q, p) = q_a - f(q_u, p_u)$ of order 1, where $f \in C^2\left(\mathcal{Q}_u \times \mathscr{P}_u; \mathcal{Q}_a\right)$. Since $\nabla_{q_u}M^{-1}(q) = 0_{2\times2}$, Theorem 2.10 tells us that this VNHC will be regular if the regularity matrix

$$dh_q M^{-1}(q)\begin{bmatrix} 0 \\ 1 \end{bmatrix},$$

is of full rank on the constraint manifold Γ. Then, since

$$dh_q = \begin{bmatrix} -\partial_{q_u}f & 1 \end{bmatrix},$$

the regularity matrix evaluates to the scalar equation

$$\frac{(1 + c_a)\partial_{q_u}f(q_u, p_u) + (3 + 2c_a)}{ml^2(2 - c_a^2)}. \tag{4.8}$$

This is full rank on Γ if and only if the numerator does not change sign.

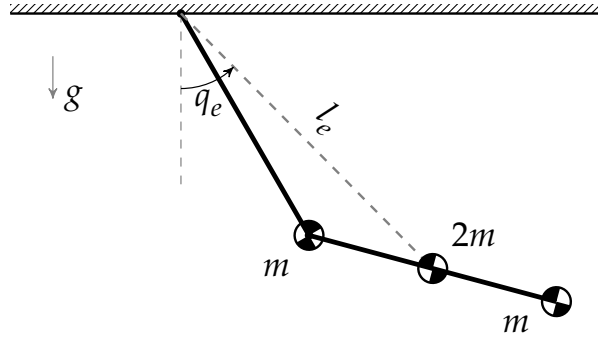A sufficient condition for regularity is when f is a function solely of p_u, because then

FIGURE 4.3: A simple acrobot modelled as a VLP with equivalent center of mass $2m$. The length of the VLP changes according to q_a.

$\partial_{q_u} f = 0$ and (4.8) is strictly positive for all values of q_a. This will be useful later, as we will not need to check regularity if we design a function of the unactuated momentum.

The acrobot is noticeably more complex than the VLP, as the dynamics of (q_u, p_u) and (q_a, p_a) are coupled through $M^{-1}(q)$. Because of this, the constrained dynamics of an arbitrary VNHC may not be easy to write out. In the rest of this chapter, our goal is to design the function $f(q_u, p_u)$ based on the natural human motion of a gymnast, with one caveat: we must be able to prove the constrained dynamics will inject energy into the acrobot.

4.3 Previous Constraint Approaches

Let us examine some of the existing approaches to generating giant motion for the acrobot, since these may be viable candidates on which to base a VNHC.

One initial approach to controlling the acrobot is to model it as a variable-length pendulum by collapsing the two rods and masses into one equivalent center of mass (ECM), as in Figure 4.3. This seems a reasonable model reduction, since the length from the pivot to the ECM changes depending on the angle q_a of the leg. Indeed, Henmi et al. [18] use this approach to design a trajectory for the ECM, then determine which leg angles $q_a(t)$ are required to generate that trajectory. Following in their footsteps, we might consider using the results from Chapter 3 to find the leg angles that allow the ECM to gain energy. Then we could apply Theorem 3.4 to prove the acrobot is gaining energy too.

Unfortunately, the VLP is not a true representation of the acrobot. The effective length of the ECM is
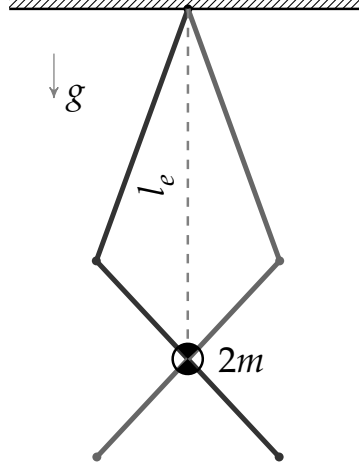
$$l_e(q_a) := l\sqrt{\frac{5}{4} + c_a},$$

FIGURE 4.4: The equivalent center of mass of the acrobot generally has two configurations which correspond to the same effective length and angle. These configurations are symmetric about the line connecting the pivot to the ECM.

and its effective angle is

$$q_e := \arctan_2 \left(s_u + \frac{1}{2} s_{ua}, -c_u - \frac{1}{2} c_{ua} \right).$$

There are two important notes to consider based on these equations. First, Figure 4.4 shows that for each pose of the VLP representation, there are two configurations of the acrobot which give the same effective length and angle. This means the acrobot and the VLP are not equivalent representations; designing a VNHC that injects energy using the ECM may not produce human-like leg motion on the acrobot.

Second, if we were to compute the conjugate of momenta p_{l_e} to l_e and p_e to q_e, we would see the torque input τ appearing in both of their dynamic equations. In the VLP model from Chapter 3, the control input only affects the dynamics of the length variable. If we want to design a VNHC for this system, we cannot use any of the results from Chapter 3 because the VLP models don't match.

Since we cannot apply the results of Chapter 3 to simplify the proof of energy injection, and the resulting ECM motion may not even produce realistic leg motion, this model reduction is ineffective for our purposes.

Let us turn next to the thesis of Wang [21], who designs a VHC to enforce a so-called "tap" motion with the purpose of injecting energy into the acrobot. First, he defines a compensator variable s which tracks $\dot{q}_u$, so that he can use the theory of VHCs with the extended configuration (q_u, q_a, s). He then finds $h_1, h_2 \in \mathbb{R}_{>0}$ to define the normalized radius ρ and normalized angle ξ in the (q_u, s)-plane. These normalized variables are

given by

$$\rho := \sqrt{h_1 q_u^2 + h_2 s^2},$$

$$\xi := \arctan_2(h_2 s, h_1 q_u).$$

He then sets the VHC to be $h(q) = q_a - f_{rad}(\rho) f_{ang}(\xi)$ with the control parameters $\bar{q}_u$ and ρ_0, where

$$f_{rad}(\rho) := \tanh^2(\rho/\rho_0), \tag{4.9}$$

$$f_{ang}(\xi) := \begin{cases} 0 & -\pi < \xi \leq 0 \\ \bar{q}_u \exp\left(1 - \frac{1}{1-(\frac{4\xi}{\pi}-1)^2}\right) & 0 < \xi \leq \frac{\pi}{2} \\ 0 & \frac{\pi}{2} < \xi \leq \pi. \end{cases} \tag{4.10}$$

While this constraint shows promising experimental results and it accurately emulates true human motion, Wang does not provide an analytical proof that the acrobot will gain energy. His lack of analysis is tied to the fact that the constrained dynamics are incredibly complicated. In fact, just showing the constraint is regular is a challenging task. While we could very easily convert his VHC into a VNHC by replacing s with p_u, we would run into the same problem. Since we want our constraint to *provably* inject energy, we must forgo this type of constraint in favour of something less complex.

4.4 The Acrobot Constraint

One may be tempted to design a constraint of the form $q_a = \bar{q}_a \sin(\theta)$ with $\theta := \arctan_2(p_u, q_u)$, since a similar approach was so effective for the VLP in Chapter 3. Unfortunately, this constraint is not regular, and it is difficult to find any VNHC of the form $q_a = f(\theta)$ where it is easy to prove regularity analytically. Instead, we will develop a constraint $h(q, p) = q_a - f(p_u)$ which, as we saw earlier, is always regular and may still be likely to inject energy.

To design this constraint, let us imagine what a human does on a seated swing. When they are moving forward they extend their legs, and when they are moving backward they retract them. In reality, the motion is slightly more complicated than that: as the swing gains speed, the person leans their body back while extending their legs. This allows them to bring their legs higher, shortening the distance from their center of mass to the pivot and adding more energy to the swing. When the swing
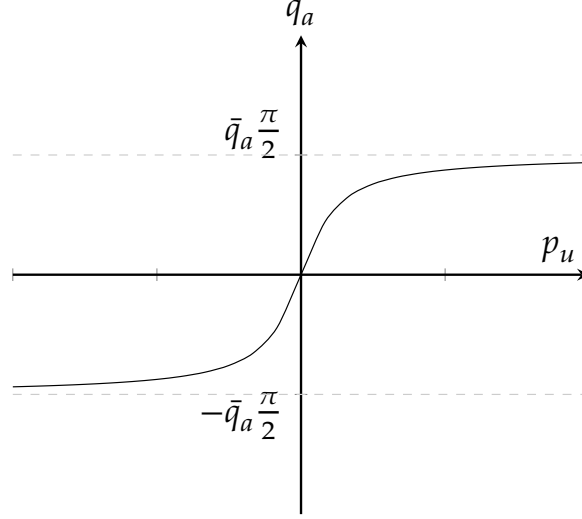
FIGURE 4.5: The acrobot constraint $q_a = \bar{q}_a \arctan_2(Ip_u)$.

moves backward, they sit up and fully retract their legs underneath them.

Now imagine we have affixed the torso of the acrobot to the swing's rope, so that the legs can pivot both forwards and backwards. The legs cannot bend, so in an attempt to emulate motion the legs should pivot in the direction of motion proportionally to the swing's speed. One VNHC which emulates this process is $q_a = \bar{q}_a \arctan_2(Ip_u)$, as in Figure 4.5. Here, $\bar{q}_a \in]0, \frac{2Q_a}{\pi}]$ so that $q_a \in [-Q_a, Q_a]$ and $I \in \mathbb{R}_{>0}$ is a fixed control parameter.

This constraint is not a perfect emulation of a gymnast's movement – during a giant the gymnast's legs are almost completely extended, while our constraint retracts the legs partially during rotations. However, the motion looks similar enough that this constraint should provide a decent foundation for injecting energy into the acrobot. It is for this reason that we choose our acrobot's constraint to be

$$h(q, p) = q_a - \bar{q}_a \arctan_2(Ip_u). \tag{4.11}$$

Let us now compute the constrained dynamics under (4.11). Note that $dh_q = \begin{bmatrix} 0 & 1 \end{bmatrix}^\mathsf{T}$, while

$$dh_{p_u} = \frac{-\bar{q}_a I}{1 + I^2 p_u^2}.$$

Applying these to (2.16), we get the solution for p_a on the constraint manifold as

$$p_a(q_u, p_u) = \frac{(1 + c_a)(1 + I^2 p_u^2)p_u - m^2 g l^3 \bar{q}_a I(2 - c_a^2)(2s_u + s_{ua})}{ml^2(3 + 2c_a)(1 + I^2 p_u^2)}.$$

The dynamics for p_u do not contain p_a, so they remain unchanged. The constrained dynamics for q_u are given by

$$\dot{q}_u = e_1^{\mathsf{T}} M^{-1}(q) \begin{bmatrix} p_u \\ p_a(q_u, p_u) \end{bmatrix}$$

which one can simplify into

$$\dot{q}_u = \frac{(1 + I^2 p_u^2)p_u - m^2 gl^3 \bar{q}_a I(2s_u + s_{ua})(1 + c_a)}{ml^2(1 + I^2 p_u^2)(3 + 2c_a)}.$$

Hence, the constrained dynamics for the acrobot under (4.11) are

$$\begin{cases} \dot{q}_u = \frac{(1+I^2 p_u^2)p_u - m^2 gl^3 \bar{q}_a I(2s_u + s_{ua})(1+c_a)}{ml^2(1+I^2 p_u^2)(3+2c_a)}, \\ \dot{p}_u = -mgl(2s_u + s_{ua}). \end{cases} \tag{4.12}$$

These dynamics do not always gain energy – we need some additional conditions on the control parameters to guarantee this is true. With these conditions, (4.11) injects energy into the acrobot, as is explained by the following Theorem.

Theorem 4.1. *Consider the simple acrobot (4.6) constrained by the regular VNHC $h(q, p_u) = q_a - \bar{q}_a \arctan(Ip_u)$. Suppose $\bar{q}_a \in {]}0, 1]$. Then there exists a small enough[1] $I \in \mathbb{R}_{>0}$ such that the VNHC injects energy. Setting $I \in \mathbb{R}_{<0}$ allows the VNHC to dissipate energy.*

Proving Theorem 4.1 requires a change of coordinates and the use of perturbation theory. The full proof is given in Chapter 4.5. We will conclude this section with a high level sketch of the proof.

The energy-based proof used in Chapter 3 does not work for the acrobot, since no "average energy" function has positive derivative everywhere for these dynamics. We instead use a perturbation analysis. When $I = 0$, the acrobot behaves like a simple pendulum with two masses. There is a suitable change of coordinates into a pseudo-radius $\mu \in \mathbb{R}_{>0}$ and pseudo-angle $\alpha \in \mathbb{S}^1$ where μ is constant along orbits of the pendulum and α is strictly increasing. We can show there exists $I > 0$ small enough such that the orbit of the acrobot in (μ, α) coordinates tracks the pendulum motion to order I. What's more, we can show that μ is increasing on average, which means the acrobot is gaining energy.

---

[1] In fact, we can be more precise than this. Letting $\epsilon > 0$, we need $I \leq \min\{I_1(\epsilon), I_2\}$ where $I_1(\epsilon) = \frac{\tan(\epsilon)}{(\pi-\epsilon)} \left(\frac{m^2 gl^3(\cos(\epsilon) - 2\sin(\epsilon))}{\pi - \epsilon} \left(\frac{2\bar{q}_a \tan(\epsilon)}{(1+\tan(\epsilon)^2)(\pi-\epsilon)} + 5 \right) \right)^{-1/2}$ and $I_2 = \sqrt{\frac{3}{10m^2 gl^3 \bar{q}_a^2}}$. See Apendix A for details.

4.5 Proving the Acrobot Gains Energy

4.6 Experimental Results

Chapter 5

Conclusion

5.1   Limitations of this Work

5.2   Future Research

Appendix A

Bounding the Acrobot Control Parameter

Bibliography

[1] F. Udwadia, "Constrained motion of hamiltonian systems," *Nonlinear Dynamics*, vol. 84, no. 3, pp. 1135 – 1145, December 2015.

[2] K. Ono, K. Yamamoto, and A. Imadu, "Control of giant swing motion of a two-link horizontal bar gymnastic robot," *Advanced Robotics*, vol. 15, no. 4, pp. 449 – 465, 2001.

[3] X. Zhang, H. Cheng, Y. Zhao, and B. Gao, "The dynamical servo control problem for the acrobot based on virtual constraints approach," in *The 2009 IEEE/RSJ International Conference on Intelligent Robots and Systems*. St. Louis, USA: IEEE, October 2009.

[4] A. Mohammadi, M. Maggiore, and L. Consolini, "Dynamic virtual holonomic constraints for stabilization of closed orbits in underactuated mechanical systems," *Automatica*, vol. 94, pp. 112 – 124, August 2018.

[5] E. Papadopoulos and G. Papadopoulos, "A novel energy pumping strategy for robotic swinging," in *2009 17th Mediterranean Conference on Control and Automation*. Thessaloniki, Greece: IEEE, June 2009.

[6] A. J. V. der Schaft, "On the hamiltonian formulation of nonholonomic mechanical systems," *Reports on Mathematical Physics*, vol. 34, no. 2, pp. 225 – 233, 1994.

[7] O. E. Fernandez, "The hamiltonization of nonholonomic systems and its applications," Ph.D. dissertation, University of Michigan, 2009.

[8] S. Wirkus, R. Rand, and A. Ruina, "How to pump a swing," *The College Mathematics Journal*, vol. 29, no. 4, pp. 266 – 275, 1998.

[9] J. Horn, A. Mohammadi, K. Hamed, and R. Gregg, "Hybrid zero dynamics of bipedal robots under nonholonomic virtual constraints," *IEEE Control Systems Letters*, vol. 3, no. 2, pp. 386 – 391, April 2019.

[10] S. C. Anco and G. Bluman, "Integrating factors and first integrals for ordinary differential equations," *European Journal of Applied Mathematics*, vol. 9, pp. 245 – 259, 1998.

[11] A. Mohammadi, M. Maggiore, and L. Consolini, "On the lagrangian structure of reduced dynamics under virtual holonomic constraints," *ESAIM: Control, Optimization and Calculus of Variations*, vol. 23, no. 3, pp. 913 – 935, June 2017.

[12] M. S. Branicky, "Multiple lyapunov functions and other analysis tools for switched and hybrid systems," *IEEE Transactions on Automatic Control*, vol. 43, no. 4, pp. 475 – 482, April 1998.

[13] J. Lu and L. J. Brown, "A multiple lyapunov functions approach for stability of switched systems," in *2010 American Control Conference*.   Baltimore, USA: IEEE, July 2010.

[14] A. M. Bloch, J. E. Marsden, and D. V. Zenkov, "Nonholonomic dynamics," *Notices of the AMS*, vol. 52, no. 3, pp. 320 – 329, March 2005.

[15] V. Sevrez, E. Berton, G. Rao, and R. J. Bootsma, "Regulation of pendulum length as a control mechanism in performing the backward giant circle in gymnastics," *Human Movement Science*, vol. 28, no. 2, pp. 250 – 262, March 2009.

[16] B. Piccoli and J. Kulkarni, "Pumping a swing by standing and squatting: Do children pump time-optimally?" *IEEE Control Systems Magazine*, vol. 25, no. 4, pp. 48 – 56, August 2005.

[17] A. D. Mahindrakar and R. N. Banavar, "A swing-up of the acrobot based on a simple pendulum strategy," *International Journal of Control*, vol. 78, no. 6, pp. 424 – 429, 2005.

[18] T. Henmi, M. Chujo, Y. Ohta, and M. Deng, "Reproduction of swing-up and giant swing motion of acrobot based on a technique of the horizontal bar gymnast," in *Proceedings of the 11th World Congress on Intelligent Control and Automation*. Shenyang, China: IEEE, June 2014.

[19] M. Maggiore and L. Consolini, "Virtual holonomic constraints for euler-lagrange systems," *IEEE Transactions on Automatic Control*, vol. 58, no. 4, pp. 1001 – 1008, April 2013.

[20] X. Xin and Y. Liu, "Trajectory tracking control of variable length pendulum by partial energy shaping," *Communications in Nonlinear Science and Numerical Simulations*, vol. 19, no. 5, pp. 1544 – 1556, May 2014.

[21] X. Wang, "Motion control of a gymnastics robot using virtual holonomic constraints," Master's thesis, University of Toronto, 2016.

[22] H. K. Khalil, *Nonlinear Systems*, 3rd ed. Upper Saddle River, NJ 07485: Prentice Hall, 2002.

[23] D. T. Greenwood, *Principles of Dynamics*, 2nd ed. Englewood Cliffs, NJ: Prentice Hall, 1987.

[24] L. D. Landau and E. M. Lifschitz, *Mechanics*, 3rd ed. Butterworth-Heinemann, January 1982.

[25] J. A. Acosta, R. ortega, A. Astolfi, and A. Mahindrakar, "Interconnection and damping assignment passivity-based control of mechanical systems with underactuation degree one," *IEEE Transactions on Automatic Control*, vol. 50, no. 12, pp. 1936 – 1955, December 2005.

[26] A. Mahindrakar, A. Astolfi, R. Ortega, and G. Viola, "Further constructive results on interconnection and damping assignment control of mechanical systems: The acrobot example," in *Proceedings of the 2006 American Control Conference*. Minneapolis, Minnesota, USA: American Control Conference, June 2006.

[27] J. Grizzle, C. Chevallereau, R. Sinnet, and A. Ames, "Models, feedback control, and open problems of 3d bipedal robotic walking," *Automatica*, vol. 50, no. 8, pp. 1955 – 1988, August 2014.

[28] F. Plestan, J. Grizzle, E. R. Westervelt, and G. Abba, "Stable walking of a 7-dof biped robot," *IEEE Transactions on Robotics and Automation*, vol. 19, no. 4, pp. 653–668, August 2003.

[29] A. Mohammadi, E. Rezapour, M. Maggiore, and K. Y. Pettersen, "Maneuvering control of planar snake robots using virtual holonomic constraints," *IEEE Transactions on Control Systems Technology*, vol. 24, no. 3, pp. 884 – 899, May 2015.

[30] L. Consolini and M. Maggiore, "Control of a bicycle using virtual holonomic constraints," *Automatica*, vol. 49, no. 9, pp. 2831–2839, September 2013.

[31] S. Westerberg, U. Mettin, A. S. Shiriaev, L. B. Freidovich, and Y. Orlov, "Motion planning and control of a simplified helicopter model based on virtual holonomic constraints," in *2009 International Conference on Advanced Robotics*. Munich, Germany: IEEE, June 2009, pp. 1–6.

[32] T. Takubo, H. Arai, and K. Tanie, "Virtual nonholonomic constraint for human-robot cooperation in 3-d space," in *2000 IEEE/RSJ International Conference on Intelligent Robots and Systems*. Takamatsu, Japan: IEEE, October 2000.

[33] S. Shibata and T. Murakami, "Psd based virtual nonholonomic constraint for human interaction of redundant manipulator," in *Proceedings of the 2004 IEEE International Conference on Control Applications*. Taipei,Taiwan: IEEE, September 2004.

[34] J. D. Castro-Díaz, P. Sánchez-Sánchez, A. Gutiérrez-Giles, M. Arteaga-Pérez, and J. Pliego-Jiménez, "Experimental results for haptic interaction with virtual holonomic and nonholonomic constraints," *IEEE Access*, vol. 8, pp. 120 959 – 120 973, July 2020.

[35] S. Vozar, Z. Chen, P. Kazanzides, and L. L. Whitcomb, "Preliminary study of virtual nonholonomic constraints for time-delayed teleoperation," in *2015 IEEE/RSJ International Conference on Intelligent Robots and Systems*. Hamburg, Germany: IEEE, October 2015.

[36] B. Griffin and J. Grizzle, "Nonholonomic virtual constraints for dynamic walking," in *2015 54th IEEE Conference on Decision and Control*. Osaka, Japan: IEEE, December 2015.

[37] J. C. Horn, A. Mohammadi, K. A. Hamed, and R. D. Gregg, "Nonholonomic virtual constraint design for variable-incline bipedal robotic walking," *IEEE Robotics and Automation Letters*, vol. 5, pp. 3691 – 3698, February 2020.

[38] W. K. Chan, Y. Gu, and B. Yao, "Optimization of output functions with nonholonomic virtual constraints in underactauted bipedal walking control," in *2018 Annual American Control Conference*. Milwaukee, USA: IEEE, June 2018.

[39] A. O. Belyakov, A. P. Seyranian, and A. Luongo, "Dynamics of the pendulum with periodically varying length," *Physica D*, vol. 238, pp. 1589 – 1597, August 2009.

[40] C. Li, Z. Zhang, X. Liu, and Z. Shen, "An improved principle of rapid oscillation suppression of a pendulum by a controllable moving mass: Theory and simulation," *Shock and Vibration*, vol. 2019, April 2019.

[41] L. Wang, W. Shi, and Y. Zhou, "Study on self-adjustable variable pendulum tuned mass damper," *The structural design of tall and special buildings*, vol. 28, January 2019.

[42] A. M. Lyapunov, "The general problem of stability of motion (in russian)," Ph.D. dissertation, University of Kharkhov, Kharkhov, Russia, 1892.

[43] J. Hauser and R. Murray, "Nonlinear controllers for non-integrable systems: the acrobot example," in *1990 American Control Conference*. San Diego, USA: IEEE, May 1990.

[44] E. Westervelt, "Toward a coherent framework for the control of planar biped locomotion," Ph.D. dissertation, University of Michigan, Michigan, USA, 2003.

[45] M. W. Spong, "The swing up control problem for the acrobot," *IEEE Control Systems Magazine*, vol. 15, pp. 49–55, February 1995.

[46] X. Xin and M. Kaneda, "The swing up control for the acrobot based on energy control approach," in *Proceedings of the 41st IEEE Conference on Decision and Control*. Las Vegas, USA: IEEE, March 2003.

[47] T. Henmi, M. Akiyama, and T. Yamamoto, "Motion control of underactuated linkage robot based on gymnastic skill," *Electrical Engineering in Japan*, vol. 206, pp. 42–50, January 2009.

[48] P. E. Pidcoe, "The biomechanics principles behind training giant swings," Online, Virginia Commonwealth University, Richmond, VA, USA, August 2005, accessed 11 September 2020. https://usagym.org/pages/home/publications/technique/2005/8/giant.pdf.

[49] G. Golub and W. Kahan, "Calculating the singular values and pseudo-inverse of a matrix," *Journal of the Society for Industrial and Applied Mathematics: Series B, Numerical Analysis*, vol. 2, no. 2, pp. 204–224, 1965.

[50] E. A. Barbashin and N. N. Krasovskii, "On the stability of motion as a whole (in russian)," *Doklady Akademii Nauk SSSR*, vol. 86, pp. 453–456, 1952.

[51] R. D. Schafer, *An Introduction to Non-Associative Algebras*. New York: Dover Publications, 1996.

[52] I. Bendixson, "Sur les courbes définies par les équations différentielles," *Acta Math*, vol. 24, pp. 1–88, 1901.

[53] L. Perko, *Differential equations and dynamical systems*, 3rd ed. New York, USA: Springer, 2013, vol. 7.